Malformations of the Spine

9

Luciana Porto

Contents

9.1 Introduction

Spinal dysraphisms are a heterogeneous group of malformations, which may involve the vertebral column and the neuroaxis. The involvement of mesodermal structures is common and variable. The focus investigating these children should lie on the neural tissues. When a malformation is found, full and detailed mapping of the entire malformation should be performed to facilitate surgical planning.

L. Porto
Institute for Neuroradiology, Goethe-University,
Schleusenweg 2-16, D-60528 Frankfurt, Germany
e-mail: luciana.porto@kgu.de

E. Hattingen et al. (eds.), *Diseases of the Spinal Cord*,
DOI 10.1007/978-3-642-54209-1_9, © Springer-Verlag Berlin Heidelberg 2015

- The conus at term birth: L2/L3. By 8 weeks, the cord has ascended to the adult level at the L1/L2 intervertebral space.
- The pediatric cervical spine is more prone to instability.

Two embryological processes are involved in the formation of the spinal cord. The upper part of the cord up to mid-lumbar enlargement occurs by neurulation. The smaller distal lumbar portion of the cord, the conus medullaris, and the filum terminale are formed by canalization and regressive differentiation. Although nervous tissue abnormalities are not always associated with musculoskeletal anomalies, congenital spine abnormalities may involve mesodermal as well as neuroectodermal structures. In the early embryonic phase, the cutaneous ectoderm is attached to the neuroectoderm. The disjunction between neural and cutaneous ectoderm is critical. If it fails, mesenchymal tissue becomes enclosed within the neural tube.

Because of the relatively rapid fetal growth in the caudal direction, the conus lies at birth at the vertebral segment L2/L3. By 8 weeks after birth, the cord has ascended to the adult level at the L1/L2 interspace.

The pediatric cervical spine is more prone to instability due to weak cervical musculature, disproportionately large head size, and incomplete ossification of the dens. In addition, the immature spine is hypermobile due to laxity of the ligaments, and it has small and thin facet joints making the atlas–axis region prone to injury. Therefore, children younger than 11 years of age are more likely to have ligamentous injuries rather than fractures of the upper cervical spine. In contrast, teenagers more often sustain injuries to the lower cervical spine. MRI is irreplaceable when evaluating "spinal cord injury without radiographic abnormality" (SCIWORA); it helps evaluating the spinal cord, discs, and ligaments.

Unfortunately, the evaluation of the pediatric cervical spine, particularly the craniocervical junction (CCJ), can be very difficult because of the presence of synchondroses, variants, and injuries that are found in this age group only. Therefore, knowledge of the anatomy is prerequisite to evaluate imaging correctly.

9.2 Craniocervical Junction Anomalies

The CCJ consists of the occipital bone, foramen magnum, clivus, atlas, axis, and the ligaments of the atlantooccipital and atlantoaxial articulations. The CCJ is, as other transitional zones, host to many variants, anomalies, and malformations; therefore, it is considered an unstable zone. The upper part (C1 and C2) is responsible for most of the rotational mobility of the cervical spine, but the cervical bones and joints are intrinsically unstable; therefore, the ligaments are structurally responsible for upper cervical stability. C1–C2 instability is present in up to 50 % of congenital atlantooccipital anomalies.

Basilar invagination is typically caused by occipital bone anomalies and atlantooccipital non-segmentation.

In case of a CCJ anomaly, important areas, such as the brainstem, spinal cord, and their arteries, can be affected and become compressed from posterior displacement of the odontoid process. The symptoms of patients with CCJ abnormalities are inconsistent. Neurological symptoms may occur late; they usually develop insidiously and progress slowly, becoming symptomatic as late as in the second or third decade of life. Since the associated C1–C2 instability progresses with age, patients show slow progression. Patients can be completely asymptomatic in the newborn period and early infancy, especially in connective tissue disorders associated with ligamentous laxity and in congenital anomalies, posing a diagnostic challenge.

Imaging

- MRI is the ideal method to evaluate the neural structures, ligaments, and soft tissues, while computed tomography (CT) can be used to evaluate the osseous structure of the CCJ. However, dose considerations limit the use of CT.
- Radiological imaging can be confounded by incomplete ossification of the bone (due at 9 years of age). Still, conventional radiographs remain the main diagnostic tool to evaluate pediatric cervical instability. Certain standards should be followed to obtain good RX in pediatric patients.
- When possible, RX should be taken sitting or standing. If supine RX is performed, the shoulders should be lifted from the table by a support (avoiding cervical hyperlordosis).
- RX should be perpendicular and taken from the farthest possible distance from the patient (min. 2.75 m).
- Lateral and open mouth odontoid views should be performed only after 5 years of age.

The atlantodens interval (ADI) is the space between anterior surface on the dens and posterior surface of anterior ring of C1 (Fig. 9.1a). ADI greater than 5 mm on lateral radiographs indicates instability; this value is higher than in adults (3 mm) because of the thicker cartilage of both the dens and the ring of C1. Still, an ADI of 5 mm or more can occur in children without disruption of the transverse ligaments. The risk of associated neurological problems is evaluated with the measurement of the space available for the cord (SAC), as measured between the posterior surface of dens and the anterior surface of the posterior arch of C1. A SAC of less than 14 mm is considered abnormal, and a value of less than 13 mm is probably an indication of cord injury. As a rule of thumb, the so-called Steel's rule of thirds can be easily applied, stating that at least one-third of the spinal canal should be left for the cord. The rule does not change during growth of the cervical spine.

Normal physiological displacement can be found in children at the level of C2–C3 and to a smaller degree at the level of C3–C4 up to 7 years of age. In addition, dentocentral synchondrosis (visible up to 11 years of age) and ossiculum terminale (appears after 5, mostly after 8 years of age) may be confused with odontoid tip fracture. Be aware that normal wedging of the C3 is seen in 7 % of younger children.

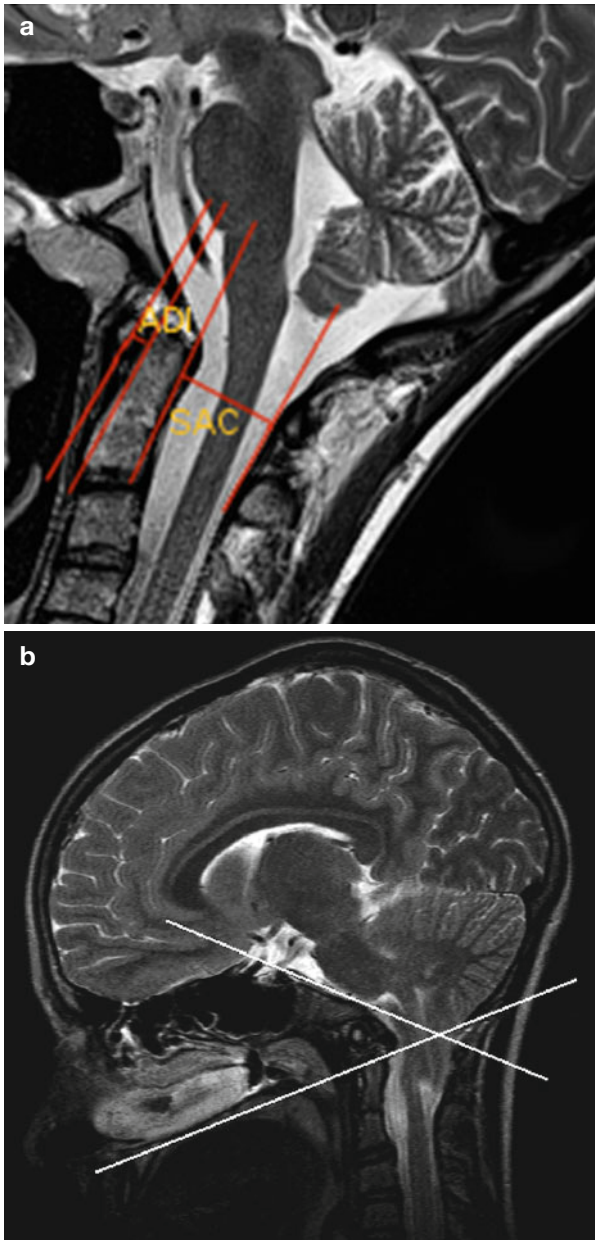

Fig. 9.1 Atlantoaxial instability and basilar invagination. (**a**) Atlantoaxial instability is determined by the atlantodens interval (*ADI*) and the space available for cord (*SAC*) (**b**): basioccipital hypoplasia associated with Chiari I malformation. There is a protrusion of the dens's tip above McGregor's line (this *line* is drawn from the hard palate to the base of the occipital bone), so-called basilar invagination with impression on the brainstem. Wackenheim's clivus baseline (which should fall tangent to the dorsal surface of the odontoid process) falls too posterior, compatible with a posterior craniocervical dislocation

- Cervical instability is frequently discovered incidentally in an asymptomatic patient
- CCJ anomalies, in particular congenital atlantoaxial dislocation, can be missed in children if not looked for.
- If trauma is not present, rule out congenital anomaly, skeletal and metabolic dystrophy, as well as rheumatoid arthritis. Typical syndromes associated with CCJ anomalies are Klippel–Feil and Down syndromes, achondroplasia, mucopolysaccharidoses, and osteogenesis imperfecta.
- Patients with connective disorders should have an MRI around 6 years of age (spine is more fully ossified and modeling has happened).
- Relative motion of more than 5 mm between anterior surface on the dens and the posterior aspect of the anterior ring of C1 indicates surgical intervention in children. This value is higher than the adults (3 mm).
- In children, a distance of less than 13 mm between posterior surface of dens and anterior surface of the posterior arch of C1 is considered abnormal.
- Basilar invagination is the protusion of dens tip more than 0.5 cm above McGregor's line. It is typically caused by occipital bone anomalies and atlantooccipital non-segmentation.
- Platibasia is the displacement of the upper cervical vertebrae with an increase of the basal angle, >150°.
- Pseudo-"physiological subluxation" at the level of C2–C3 and to a smaller degree at the level of C3–C4 is normal findings up to 7 years of age.

In general, the best diagnostic clue in imaging (MRI and/or CT) for CCJ anomalies is the flattening or malformation of the clivus, anterior ring of C1, or odontoid process. Flexion–extension MRI is often necessary to fully evaluate the pathology.

Chen and Liu (2009) described a simplified classification for malformations of the CCJ, as follows:

- Malformations of the occipital bone
- Platybasia
- Basilar invagination (basioccipital hypoplasia)
- Condylar hypoplasia
- Condylar dysplasia
- Malformations of the atlas
- Occipital atlas assimilation
- Aplasia and hypoplasia of the atlas
- Atlas arch anomaly
- Malformations of the axis and odontoid process

- Aplasia or hypoplasia of the dens
- Persistent ossiculum terminale
- Os odontoideum
- Klippel–Feil anomaly
- Instability associated with childhood diseases
  - (a) Down syndrome
  - (b) Neurofibromatosis
  - (c) Juvenile rheumatoid arthritis
  - (d) Mucopolysaccharidoses
  - (e) Achondroplasia
  - (f) Osteogenesis imperfecta
  - (g) Spondyloepiphyseal dysplasia
  - (h) Larsen syndrome
  - (i) Others

9.2.1 Malformations of the Occipital Bone

- Platybasia
- Displacement of the upper cervical vertebrae with an increase of the basal angle (normal <150°)
- Basilar invagination
- Refers to the cranial displacement of the foramen magnum with radiological protusion of the dens tip more than 0.5 cm above McGregor's line

The lower part of the clivus is formed by the basiocciput, and malformations of the occipital bone, such as basioccipital hypoplasia (Fig. 9.1b), can cause platybasia, basilar invagination (upward migration of the cervical spine into the foramen magnum), condylar hypoplasia, and condylar dysplasia. *Platybasia* can cause bony impingement on the brainstem (Fig. 9.1b) and obstructive hydrocephalus if it is associated with basilar invagination. Basilar *invagination* is associated with not only platybasia but also occipitalization of C1, fused upper vertebrae, Klippel–Feil syndrome, Chiari malformation (Fig. 9.1b), and skeletal dysplasias, mainly achondroplasia. In children, due to the greater laxity of the cervical spinal ligaments, basilar invagination can be attributable to trauma or bone softening (Fig. 9.2), as, for example, in rheumatoid arthritis. Other diseases with potential risk for basilar invagination are osteoporosis, hyperparathyroidism, osteomalacia, rickets, renal osteodystrophy, and Hurler syndrome.

Wackenheim's clivus baseline is useful for assessment of cervical instability in children with Down's syndrome and also in the assessment of traumatic injuries.

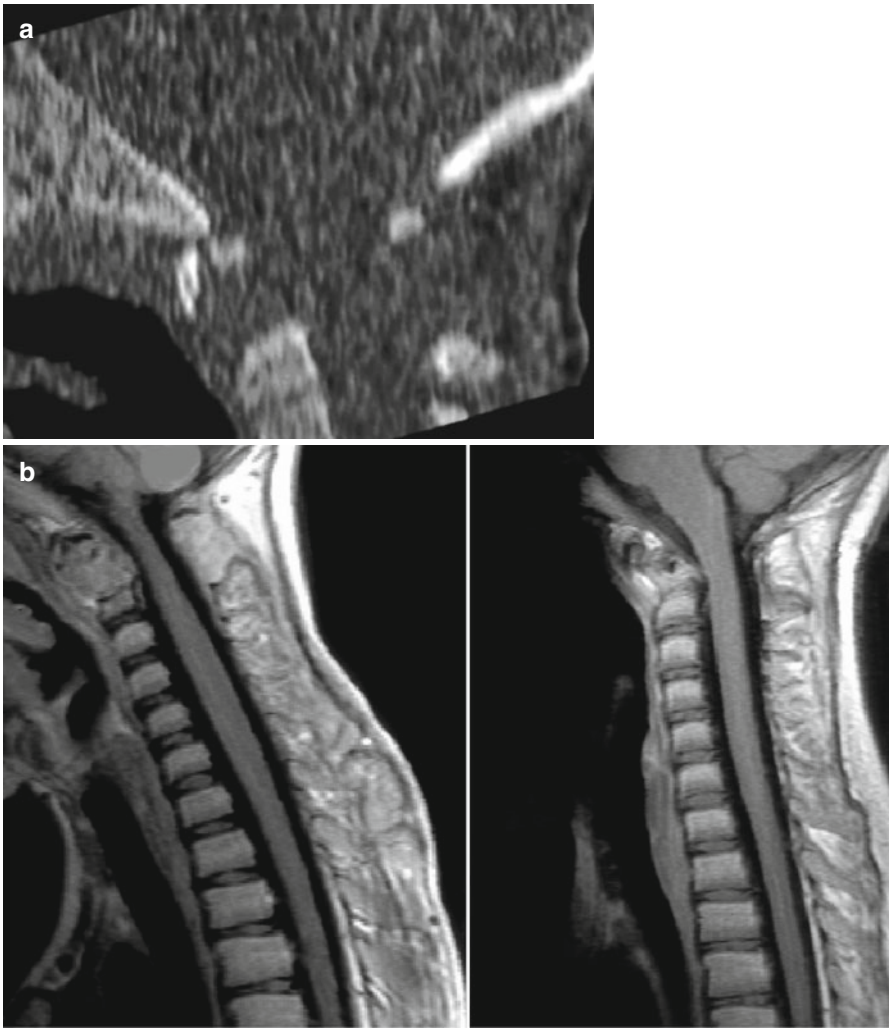

Fig. 9.2 Farber disease, a very rare lysosomal storage disease due to defective ceramidase causing accumulation of lipids leading to abnormalities in the joints, liver, throat, tissues, and central nervous system. (**a**) Sagittal CT shows a soft tissue mass eroding much of the dens axis (C2) pre-transplant. (**b**) T1-w after contrast before (*left image*) and after (*right image*) bone marrow transplantation. There is a large soft tissue mass (C2 level) which extends into the spinal canal. Note the skin nodules over spinous processes pre-transplant. *Right image*: clear improvement after therapy

It runs from the posterior surface of the clivus and normally is tangential to the posterior margin of the dens. If the line falls far of the posterior limits of the odontoid, a posterior dislocation is present. If the line intersects the anterior or middle body or the base of the odontoid, an anterior dislocation is diagnosed (Fig. 9.3).

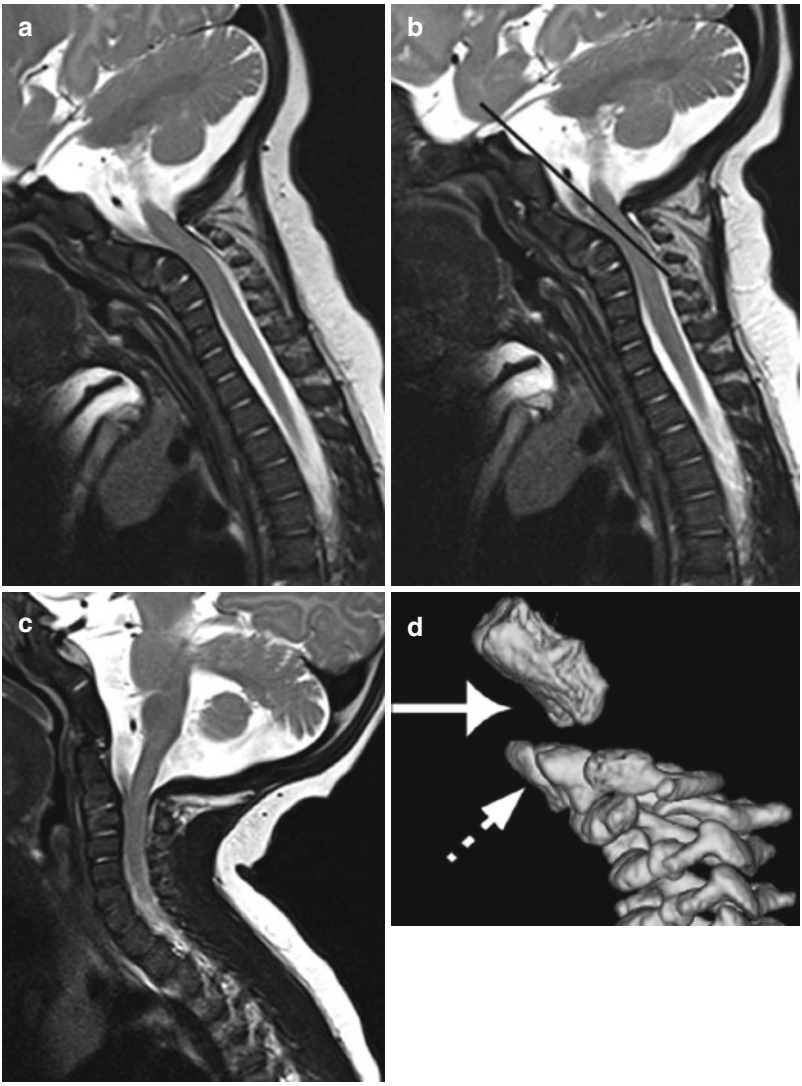

Fig. 9.3 Newborn child with incidental finding: atlantodental occipital subluxation. (**a**) Midsagittal T2-w MRI in flexion. The MR image best reveals the narrow spinal canal with compression of the spinal cord at the C1–C2 level, especially in anteflexion. (**b**) Midsagittal T2-w image in neutral position. The Wackenheim's clivus baseline intersects the body of the odontoid, well matched with an anterior craniocervical dislocation. (**c**) Midsagittal T2-w image in extension. Note that the narrowing of the spinal canal at the C1 level in flexion and neutral positions reduces in extension. (**d**) The CT scan with 3D sagittal reconstruction at the time of presentation showed an anterior displacement of unfused dens (*dotted arrow*) relative to the occipital condyles (*straight arrow*). Note the two separate ossification centers of the odontoid, so-called bifidus; normally the ossification centers fuse by the 7th fetal month. (**e**) CT scan with 3D coronal reconstruction. The neural arch is present (*star*) but unfused posteriorly. (**f**) CT scan with sagittal reconstruction. Notably, the anterior arch is not ossified in this child, which is the case in 80 % of the newborns. Besides, no unification of the posterior synchondrosis of the spinous processes is seen, which is also normal for a newborn. Therefore, during the newborn period, it is difficult to evaluate malformations, such as atlas hypoplasia, or more specifically hypoplasia of a non-united posterior arch, due to the lack of ossification, presence of synchondroses, and variants. As a differential diagnosis, one should include traumatic delivery. A control evaluation at 3 years of age is necessary

Fig. 9.3 (continued)

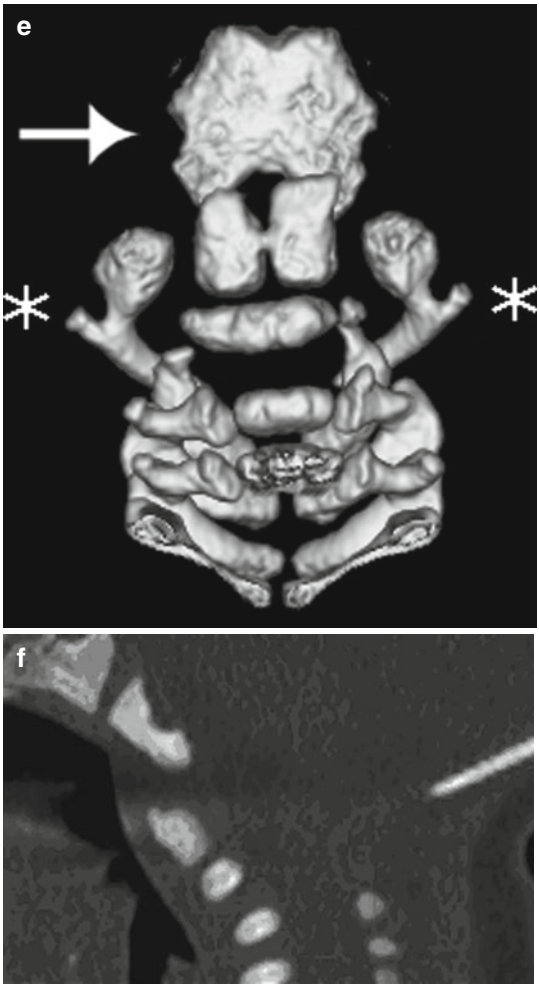

9.2.2 Malformations of the Atlas

- Due to failures of chondrogenesis, the majority of atlas anomalies are posterior arch anomalies.
- Rachischisis: Cleft of the posterior arch located in the midline, found in ca. 4 % of autopsies and in 70 % of children with myelomeningoceles

In children, the knowledge of atlas ossification centers is essential to the diagnosis of clefts, aplasias, and hypoplasias. The atlas has three ossifications sites: its anterior arch and the two neural arches. The anterior arch is ossified at birth in 20 % of children only. Usually, it becomes visible as an ossification center by 1 year of age (varying between 6 months and 2 years). During the 7th fetal week, the neural arches appear. The posterior synchondrosis of the spinous processes unites by 4–6 years of age. The complete fusion of the anterior and neural arches (neurocentral synchondrosis) does not happen before 7 years of age.

Clefts of the atlas arches are more frequent, compared to arch aplasia and hypoplasia. The greatest part of posterior arch clefts is located in the midline (rachischisis). In contrast, anterior arch rachischisis is exceptional, only found in 0.1 % of autopsies. Importantly, clefts of the anterior arch may be a sign of dysraphic anomaly of the meninges and spinal cord. Even though most of the atlas's clefts are incidental findings, its presence may be associated with other malformations of the spine, and more importantly, large clefts with fibrous tissue may present with atlas instability.

Occipital assimilation of the atlas results from a segmentation failure between the skull and the first cervical vertebra, also known as occipitalization of the atlas. The assimilation may involve the anterior arch only, the posterior arch, or both combined. This anomaly is reported as the most common anomaly involving the CCJ, encountered in 0.14–0.25 % of the population. It is always linked to basilar invagination, and there is an increased association to Klippel–Feil anomaly in C1 and C2. In this constellation, atlantoaxial subluxation and dislocation may occur. In an excellent overview, Smoker et al. describe that with the exception of the previously described atlantooccipital assimilation, most of atlas anomalies, when isolated, are not associated with abnormalities of the CCJ.

Half-sided pathology of C1 varies from *hypoplasia* of the lateral mass, up to complete agenesis of the hemiatlas with rotatory instability and basilar impression. In two-thirds of the patients, symptoms are present at birth; others show torticollis later. Partial hemiaplasias may simulate fractures on RXs.

9.2.3 Malformations of the Axis and Odontoid Process

The axis is formed by four ossification centers: one for the odontoid process, one for the body, and two for the neural arches. The odontoid process is formed in utero from two separate ossification centers which fuse by the seventh fetal month (Fig. 9.3d). The body of the axis fuses with the odontoid process around 3–6 years of age. Between 3 and 6 years of age, a secondary ossification center appears at the apex of the odontoid process (os terminale), and fusion of the os terminale with the odontoid process is completed by the age of 12 years.

By 2–3 years of age, the neural arches fuse posteriorly; their fusion to the body of the odontoid process happens between 3 and 6 years of age.

The most frequent congenital anomaly of the axis is malformation of its odontoid process, and this is not associated with basilar invagination. The malformations of the odontoid process range from mild *hypoplasia to complete aplasia*. In odontoid

hypoplasia, a short odontoid process can be recognized. Complete aplasia is particularly uncommon. The presence of a hypoplastic odontoid can be associated with spondyloepiphyseal dysplasia, mucopolysaccharidoses, and metatropic dwarfism. In the rare case of hypoplasia or aplasia, there is a predisposition to atlantoaxial dislocation with cord compression due to the absence of the apical and alar ligaments. Secondary to the hypermobility, patients may present with pannus similar to that seen in rheumatoid arthritis. In addition, there is an association with metatropic dwarfism, spondyloepiphyseal dysplasia, and Morquio syndrome.

The *ossiculum terminale* at the tip of the dens appears between 5 and 8 years and fuses to the dens between 10 and 13 years. The failure of fusion of the terminal ossicle with the rest of the odontoid process is called persistent ossiculum terminale.

- Os odontoideum
- Independent osseous structure located cranially to the axis body with a gap between these two structures. Usually a small hypoplastic dens is present.
- Persistent ossiculum terminale.
- Failure of fusion of the terminal ossicle with the rest of the odontoid process.

When isolated, the persistent *ossiculum terminale* is a stable anomaly and of little clinical significance. In contrast, *os odontoideum* (Fig. 9.4) is associated with a number of congenital conditions, such as Down and Morquio syndromes, spondyloepiphyseal dysplasia, Klippel–Feil anomaly, and Laron syndrome. If the os odontoideum is associated with ligament weakness, patients present with atlantoaxial instability (Fig. 9.4) with compression of the spinal cord. The hypermobility at C1–C2 level may cause transient occlusion of the vertebral artery. Patients with a gap between the os odontoideum and the axis body should be carefully assessed with flexion and extension examinations (Fig. 9.4).

Atlantoaxial rotatory subluxation (Fig. 9.5) in children occurs often after a minor trauma; other causes include surgery of the head and neck, following an infection or inflammation of the adjacent neck tissues. Consider anatomical variations in the differential diagnosis, i.e., children with normal atlantoaxial articulation fixed in a vicious rotatory position due to extreme torticollis (Fig. 9.6c). Clinically, children with rotatory subluxation present with new torticollis because of pain. Fortunately, most of the atlantoaxial subluxation resolves spontaneously. But, if an unresolved subluxation remains untreated, plagiocephaly may follow.

Klippel–Feil syndrome (Fig. 9.6) is a rare condition characterized by the congenital fusion of any 2 of the 7 cervical vertebrae. It is the result of a failure of the vertebrae's segmentation.

Be aware that fusion can be missed in infancy due to the incomplete ossification.

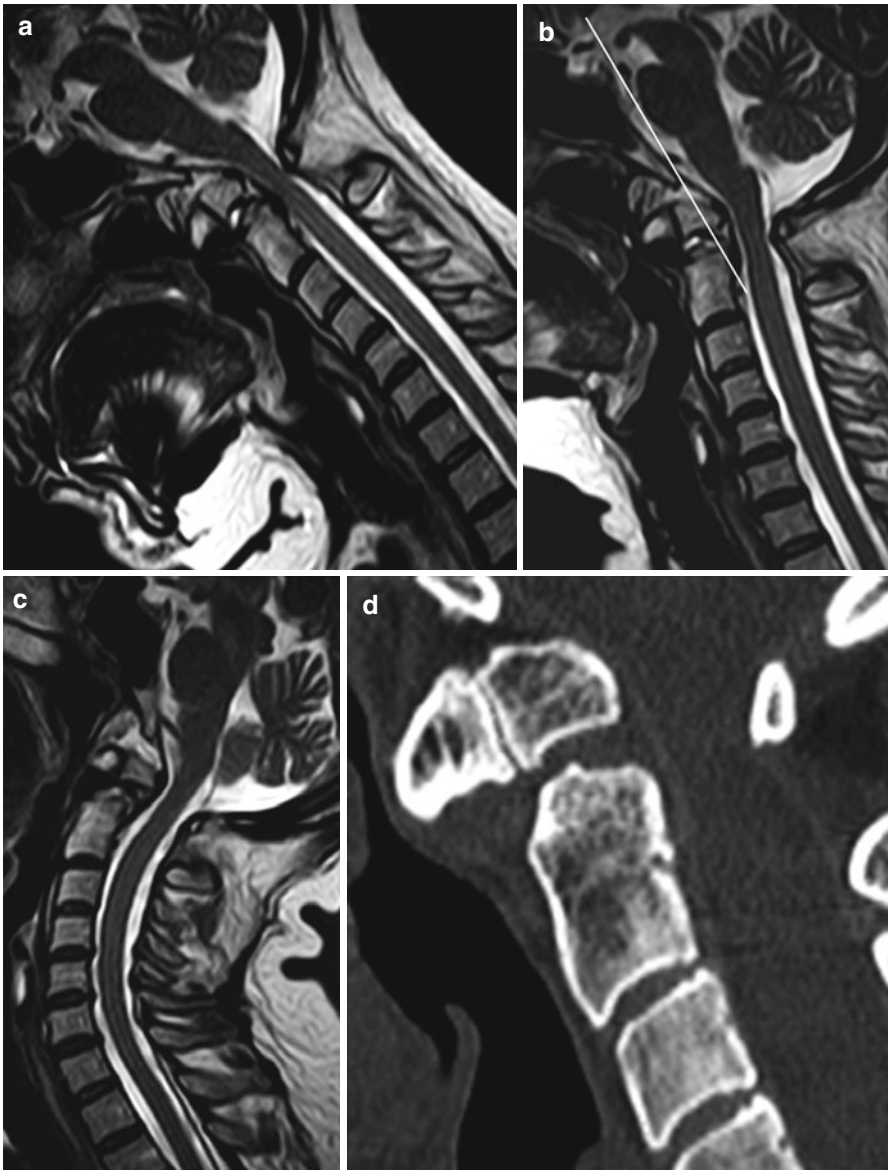

Fig. 9.4 Older patient with os odontoideum and atlantoaxial instability. (**a**) Midsagittal T2-w image in flexion. The MR image best shows the narrowing of the spinal canal with compression of the spinal cord at the C1–C2 level. (**b**) Midsagittal T2-w image in neutral position. The Wackenheim's clivus baseline intersects the body of os odontoideum, compatible with an anterior craniocervical dislocation. (**c**) Midsagittal T2-w image in extension. The narrowing of the spinal canal at the C1 level in flexion positions reduces in extension. (**d**) The CT scan shows the os odontoideum as an independent osseous structure located cranially to the axis body with a gap between these two structures. Note the presence of small hypoplastic dens

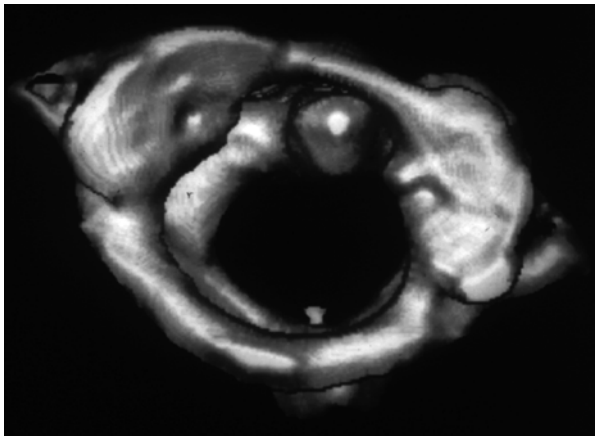

Fig. 9.5 Traumatic atlantoaxial rotatory luxation after a car accident. In children, the greater laxity of the cervical spinal ligaments results in more frequent high cervical cord injury

The patient usually presents with a short neck, low posterior hairline, and limited cervical motion.

Classification

- Type 1 (9 %): Extensive cervical and thoracic segmentation anomalies
- Type 2 (84 %): Fusion of 2 or more cervical vertebrae
- Type 3 (7 %): Type 1 or 2 associated with lower thoracic/lumbar anomalies

Approximately 20 % of the patients have a complete or partial diastematomyelia (Fig. 9.6b). Other associated abnormalities may include basilar invagination, odontoid hypoplasia, atlantooccipital assimilation, platybasia, Chiari I, scoliosis, kyphosis, Sprengel's deformity of the scapula with a bridging omovertebral bone, spina bifida, Dandy–Walker, malformations of the kidneys and the ribs, cleft palate, respiratory problems, and heart malformations. There is an increased likelihood for early instability of the CCJ in patients with atlantoaxial fusion or odontoid hypermobility associated with occipitalization of the atlas or with multiple fusion of the cervical vertebrae associated with anomalies of the atlas and odontoid process. It is important to look for instability, progressive degenerative changes, and brainstem compression.

9.2.4 Instability Associated with Representative Inherited Syndromes

9.2.4.1 Down Syndrome

In Down syndrome, a combination of osseous anomalies and lax ligaments contributes to C1–C2 instability. Patients usually present with hypoplasia of the dens without soft tissue dens mass. The prevalence of cervical instability has been estimated at 9–30 % in children with Down syndrome, although only 2.5 % of the patients present with symptomatic instability. This small group, however, has a higher

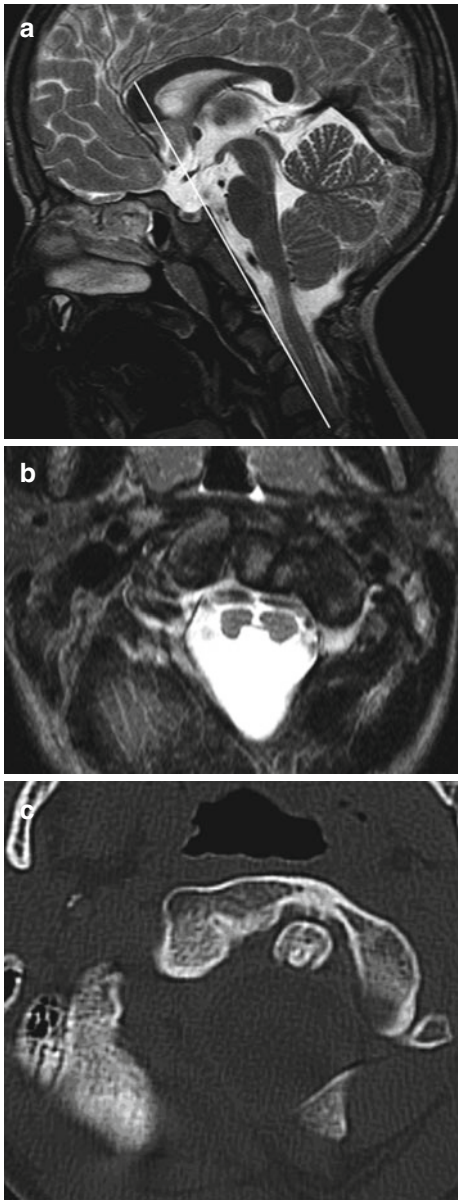

Fig. 9.6 Klippel–Feil syndrome associated with diastematomyelia. (**a**) Sagittal T2-w image shows multiple segmentation anomalies with congenital fusion. In this patient, there are associated anomalies of the atlas and odontoid process with instability of the CCJ. The Wackenheim's clivus baseline falls far too posterior to the odontoid, compatible with a craniocervical dislocation. (**b**) Almost complete split of the cord into two hemicords within a single dural sac (type II diastematomyelia). No osseous or fibrous septum was seen. (**c**) In the CT images, note the vicious rotatory position of atlanto-axial articulation due to extreme torticollis in this patient with Klippel–Feil syndrome

prevalence of associated bone abnormalities, such as os odontoideum, persistent synchondrosis, or posterior rachischisis. As a general rule, children with Down syndrome show no major compression symptoms of the spinal cord. Patients usually present with slowly progressive neurological symptoms, which can eventually lead to a main injury.

Instability can be easily evaluated using Wackenheim's clivus baseline. According to the literature, children with Down syndrome who have no C1–C2 instability will not develop a dangerous instability. Therefore, this group of patients will not need further screening after the age of 10 years. Be aware that this cutoff age can be controversial.

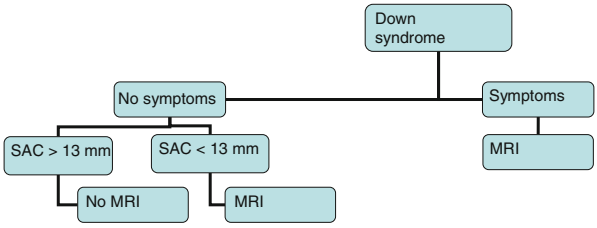

9.2.4.2 Neurofibromatosis

Neurofibromatosis can present with dystrophic changes in the vertebral bodies and dysplasia of vertebral bodies; abnormalities can also be secondary to pathological alignment. Furthermore, patients may present with focal or acute kyphoscoliosis. RX is important to quantify and to follow-up the scoliosis, while MRI is the ideal method to evaluate cord compression and nerve pathology in patients with severe cervical kyphosis. Although instability is rare, the strategy is similar as in the diagram above for Down's syndrome.

9.2.4.3 Juvenile Rheumatoid Arthritis

Juvenile rheumatoid arthritis is an important differential diagnosis to CCJ variants and anomalies.

Rheumatoid arthritis (Fig. 9.7) is a systemic disease characterized by persistent synovitis, which can affect the joints of the cervical spine.

The incidence of cervical involvement ranges from around 40 to 80 % of cases, depending on the duration of the disease. Typically, the cervical spine is involved in the beginning of the disease and shows erosive synovitis, ligamentous subluxation, osteopenia, and vertebral fractures. Patients usually develop C1–C2 subluxation within 2 years of disease onset, and spontaneous clinical remission is uncommon.

Imaging

Patients usually present with enhancing "pannus" best seen on T1-w MRI (Fig. 9.7). C1–C2 subluxation is best seen with CT reconstructions. To evaluate instability, dynamic flexion–extension plain films or T2-w MRI are invaluable.

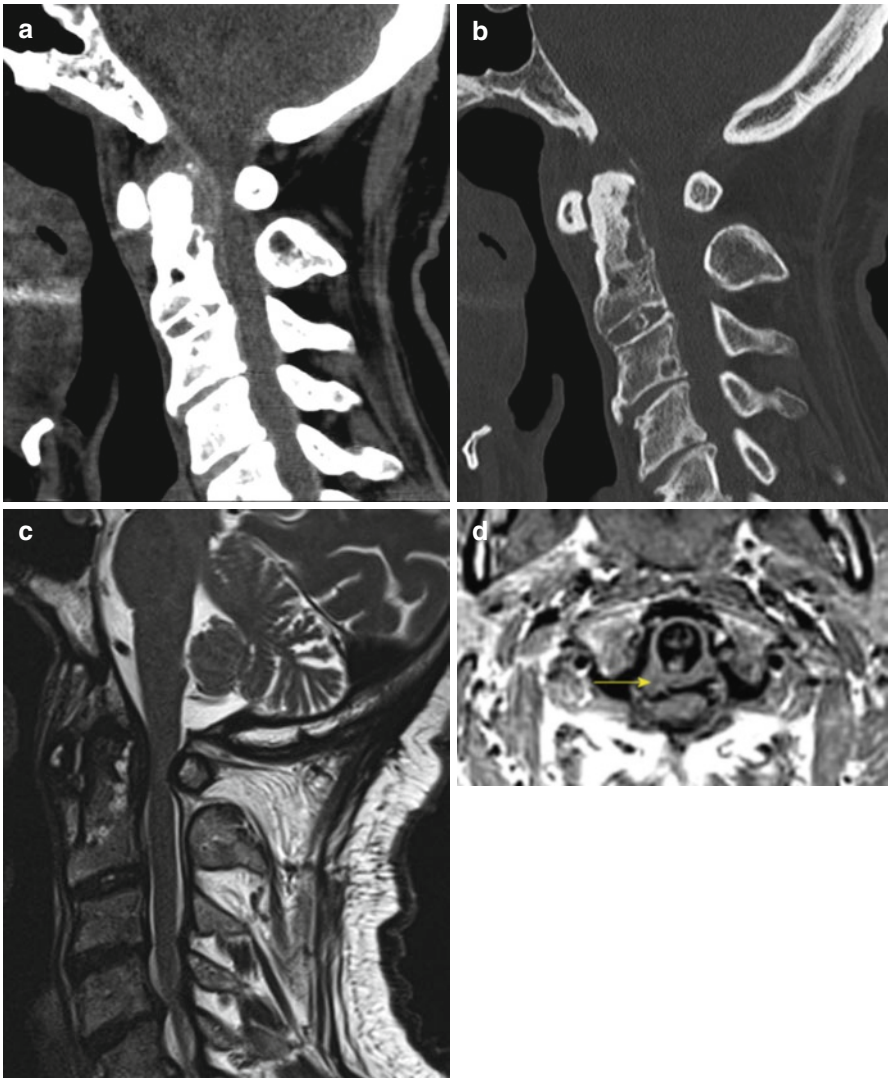

Fig. 9.7 Older patient with rheumatoid arthritis with cervical involvement. (**a**, **b**) Atlantoaxial joint CT in sagittal reformatted images: gross bone erosions of odontoid process and synovial joints, associated with joint instability (**c**, **d**) Sagittal T2-w and axial T1-w images, respectively, show the synovial pannus (*yellow arrow*) and cord compression by the odontoid process. MRI can assess the relationship of the occiput, atlas, and axis, and it is useful in depicting the extent of subluxation and the compression of the spinal cord

9.2.4.4 Mucopolysaccharidoses

Deformities of the spine are caused by deposits of glycosaminoglycans in the tissues surrounding the spinal cord, which can result in spinal cord compression. In

the case of mucopolysaccharidosis IV, also called Morquio syndrome, the "os odontoideum" is invariably present; this is due to a partially cartilaginous dens. On top, the anterior ring of C1 can be unstable because of failure in the ossification process. All these components associated with pannus lead to C1–C2 instability classically described in Morquio syndrome. However, odontoid hypoplasia and associated soft tissue thickening have been shown to reverse after bone marrow transplantation.

In Hurler syndrome (MPS 1H), another type of mucopolysaccharidosis, narrowing of the craniocervical junction, thickening of the dura mater, and odontoid dysplasia are seen (Fig. 9.8). It seems that stem cell transplantation has an early and positive impact in children with Hurler syndrome and narrowing of the craniocervical junction, influencing the development of the odontoid.

9.2.4.5 Achondroplasia

Achondroplasia is a condition characterized by short-limbed dwarfism with affection of the spine. Areas with endochondral ossification are affected, and, therefore, the skull base and foramen magnum are underdeveloped. The small foramen magnum shows a typical "teardrop" configuration, and the odontoid is usually dysplastic. Patients can also present with basiocciput hypoplasia, decrease of the basal angle, and thickening of the posterior rim of the foramen magnum.

9.2.4.6 Osteogenesis Imperfecta

Osteogenesis imperfecta is a disorder of collagen with secondary bone fragility. Patients can present with CCJ deformity, which is usually asymptomatic. As a result of recurrent microfractures, infolding of the occipital condyles can occur, leading to cranial settling with platybasia and basilar invagination. In this scenario, brainstem or lower cranial nerves compression is to be expected.

9.2.4.7 Spondyloepiphyseal Dysplasia

Atlantoaxial instability may occur due to odontoid hypoplasia or os odontoideum, resulting in cervical myelopathy.

9.2.4.8 Larsen Syndrome

Larsen syndrome is a rare defect of connective tissue formation characterized by multiple joint dislocations. Spinal anomalies may lead to major spinal instability and spinal cord injury. Atlantoaxial instability is a rare finding in this syndrome and has been reported with other abnormalities of the upper cervical spine including basilar impression and occipitalization of the atlas.

9.2.4.9 Others

Additional causes of cervical instability in children include connective tissue disorders as, for example, Ehlers–Danlos syndrome and inflammatory diseases, such as oropharyngeal infections.

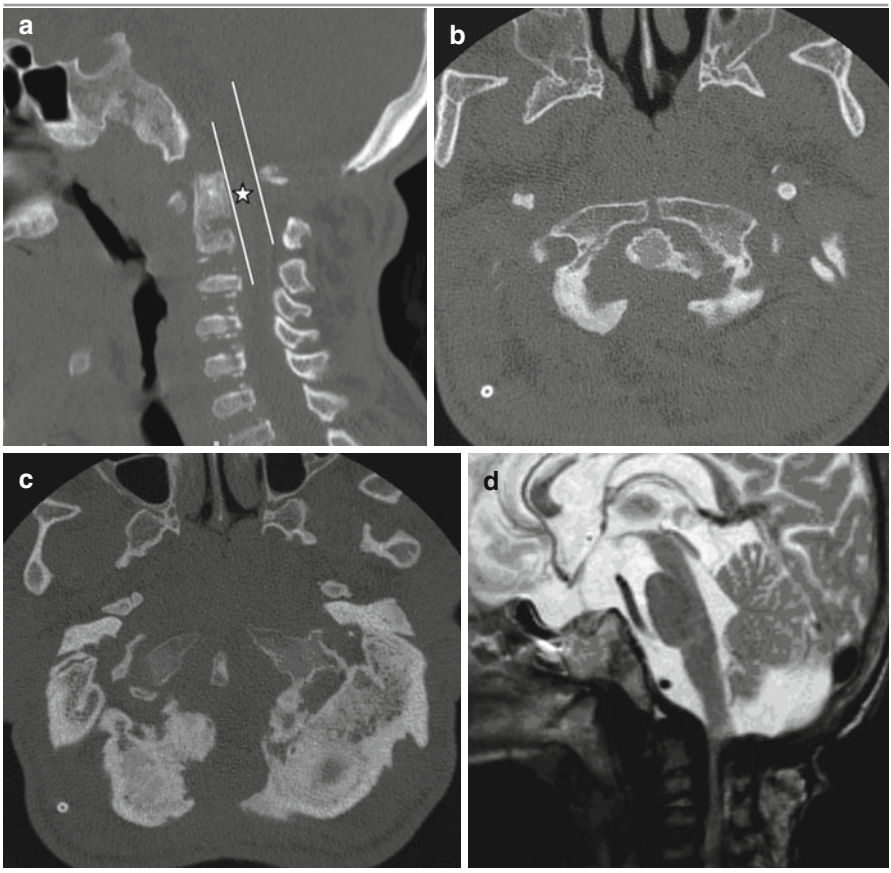

Fig. 9.8 Child with Hurler syndrome (courtesy from Prof. Lanfermann). (**a**–**c**) Notice the odontoid process is poorly developed with a short C1 posterior arch. SAC (*star*): Note the reduced available space for the cord. (**d**) Associated atlantoaxial instability. Note the typical mucopolysaccharidosis related changes: dilated Virchow–Robin spaces with involvement of the corpus callosum, frontal bossing, and a large J-shaped sella turcica. The Wackenheim's clivus baseline intersects the odontoid anteriorly, well matched with a craniocervical dislocation. In addition, meningeal hypertrophy at C2 level with clear compression of the CCJ and a smaller SAC than expected on the CT scan. The Steel's rule of thirds is violated; less than one-third of the spinal canal is left for the cord

9.3 Spina Bifida

Spinal, usually posterior defect

There are two types: closed and open

- Closed spinal dysraphism (CSD): spina bifida occulta, neural tissue covered by skin, often occurs at levels L5 and S1.
- Open spinal dysraphism (OSD): neural tissue exposed to the environment (myelomeningocele and myelocele).

- Meningocele: large opening of the spinolaminar arch with extrusion of a portion of the meningeal sac, not including the spinal cord.
- Myelomeningocele: large opening of the spinolaminar arch with extrusion of a portion of the meningeal sac with exposure of the neural placode.

Spinal dysraphisms result from an incomplete midline closure. The term spina bifida (Latin: "split spine") relates to a developmental congenital disorder caused by the incomplete closing of the osseous elements of the vertebral canal. Some vertebrae overlying the spinal cord are not fully formed and remain unfused and open. The causes of the neural tube defects are multifactorial. Environment and demographics may play a significant role in predisposing the fetus to a neural tube defect, with several studies showing the link between folic acid deficiency and neural tube defects. Methylenetetrahydrofolate reductase mutations are, for example, associated with abnormal folate metabolism predisposing to open spinal dysraphism (OSD). Additional associations are trisomy 13 and 18.

Imaging

When examining the pediatric patient, it is important to consider the radiation dose. Computed tomography of the spine has a high dose of radiation to the gonads, particularly in females. Therefore, its use should be restricted and carefully evaluated for every individual case. Neurosonography is a good initial imaging modality to evaluate the spinal canal; unfortunately, this method is limited to the neonatal period (up to 3 months) and is very operator dependent, leading to low sensitivity. Still, neurosonography has a clear role in the preliminary evaluation of a suspected spinal malformation; it gives a general idea of the position of the conus and possibly the extent of intraspinal structures, such as lipomas or cysts (Fig. 9.9).

Bony Spine

To evaluate skeleton anomalies, one should start with plain films. CT can be invaluable to understand the complex bone anatomy of segmentation anomalies, particularly in the presence of severe malformations with scoliosis (Fig. 9.10).

It is extremely important to rule out tethering of the cord prior to correction in case of segmentation anomalies with hemivertebrae and block vertebrae. In the same way, scoliosis may be caused by diastematomyelia or other forms of closed spinal dysraphism, requiring preoperative investigation of the spinal cord.

Neuroradiological investigation of the spinal canal and its contents:

MRI is the method of choice: (1) for diagnosis and determining the extent of the malformation, (2) for evaluation of the nerve roots and possible adhesions, and (3) to identify associated variants, i.e., to rule out possible surgical difficulties.

Routine: T1-w spin echo sequences and T2-w MRI, in sagittal and axial planes without contrast.

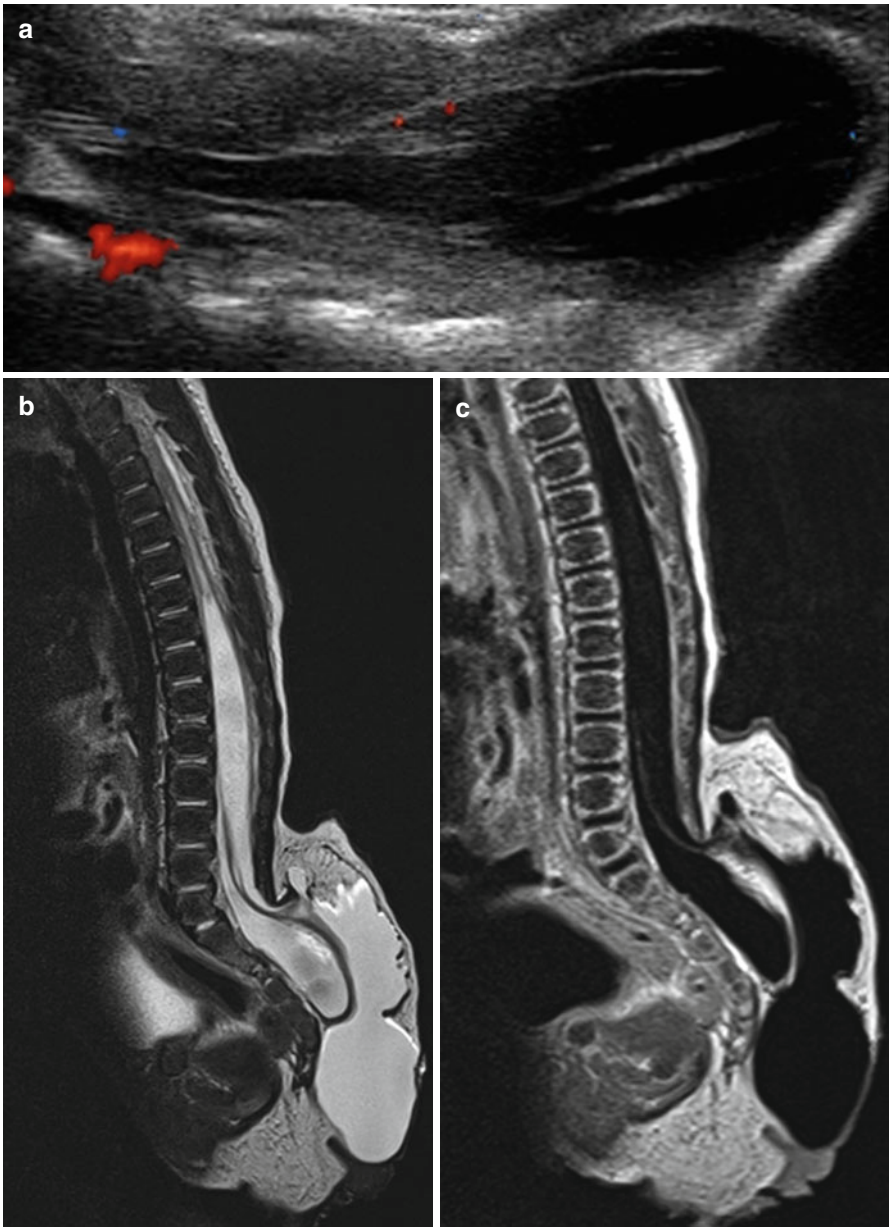

Fig. 9.9 Terminal myelocystocele. (**a**) The US imaging, corresponding to the MRI (9B), shows closed marked cystic dilatation of the distal cord central canal or the ventriculus terminalis. (**b**) Axial T2-w image shows a dilatation of the distal central canal with herniation through a posterior lumbosacral defect. (**c**, **d**) Sagittal T2-w and T1-w images, respectively, show a disruption of the mesenchyme, but not of the ectoderm, with tethered cord

Fig. 9.9 (continued)

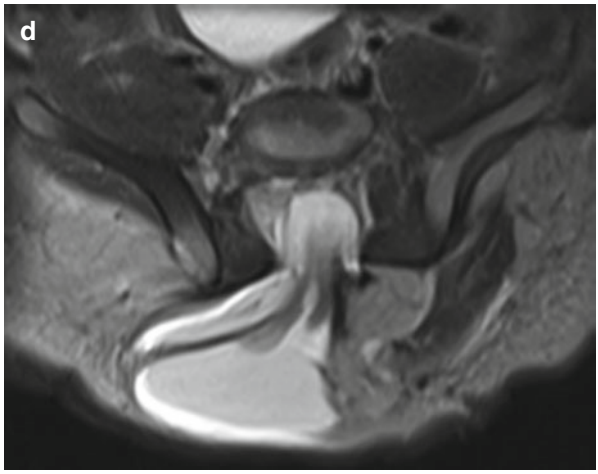

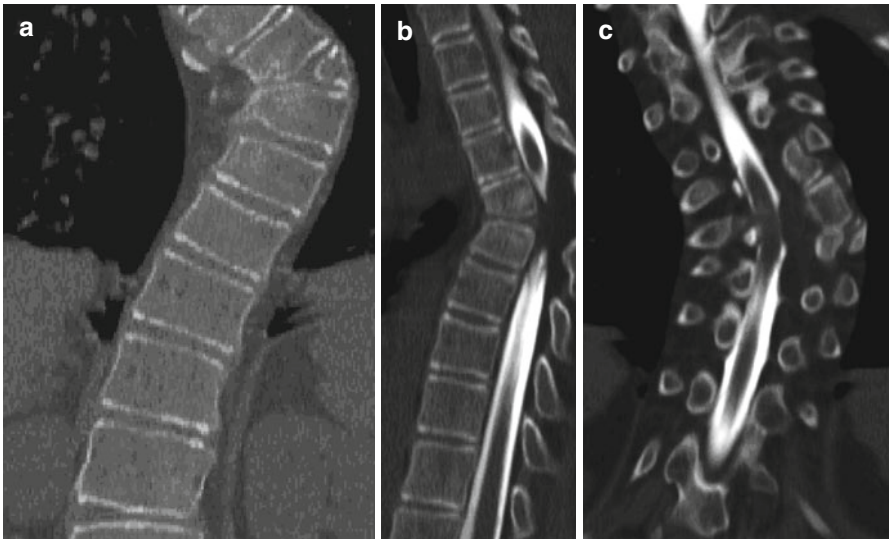

Fig. 9.10 Myelography followed by CT scanning in a patient with severe scoliosis caused by hemivertebrae with displacement of the cord. (**a**) Bone window CT scan with coronal reconstruction. (**b**, **c**) Myelography

Additional imaging: fat-suppression sequences may be useful in lipomas. Heavily T2-w multislice or single-slice MR myelography may be helpful in demonstrating the sac content with myelographic effect of the hyperintense CSF. If a spinal tumor is identified or infection is suspected, contrast should follow.

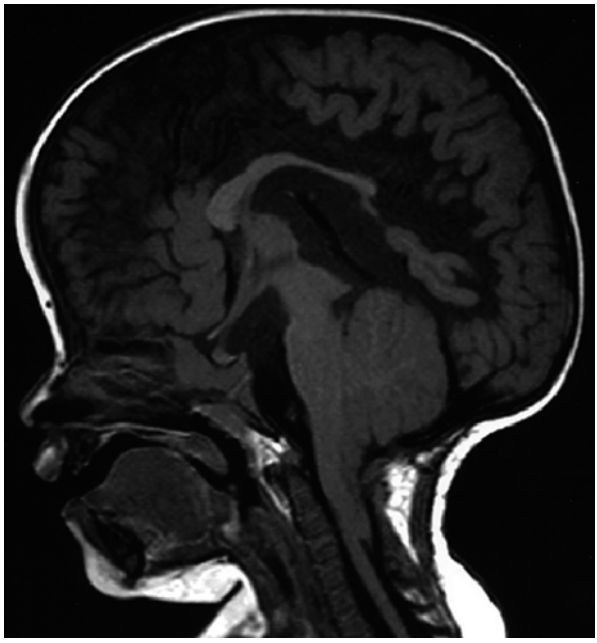

Fig. 9.11 Chiari II malformation. Sagittal T1-w image shows the typical posterior fossa deformities with small posterior fossa, low-lying tent, caudalization of the medulla. The cervicomedullary kink can be seen. The corpus callosum is dysplastic; there is a large mass intermedia, a beaked tectum of the midbrain. Note the multiple small malformed gyri (stenogyria)

In cases of severe curvature of the spine, the MRI interpretation can be difficult, and a combined evaluation with CT and CT reconstruction is advisable. In exceptional, complex cases with severe deformity, the use of myelography followed by CT scanning can be helpful (Fig. 9.10). The role of the neuroradiologist is to show all components of the malformation in detail, preparing the neurosurgeon for reconstructive surgery.

There are fundamental differences between CSD and OSD. Open spinal dysraphism is strongly associated with Arnold–Chiari II malformation (85–100 %), which is a cerebral dysgenesis characterized by a small posterior fossa. This is simply explained by the association between Chiari II malformation and the leakage of CSF through the spinal defect. The outflow (leak) collapses the primitive ventricular system, preventing the increase of the rhombencephalic vesicle and resulting in a small posterior fossa with cerebellar tonsil herniation (Fig. 9.11). The associated Arnold–Chiari II (Fig. 9.11) may be of varying degree. In the majority of cases (90 %), it is associated with hydrocephalus. Hydrocephalus may develop secondarily to mechanical obstruction due to Chiari II malformation and/or impaired CSF reabsorption. Hydrocephalus may develop in the second trimester of pregnancy, after birth, and sometimes it is seen only after the repair of meningomyelocele. Myelomeningoceles account for more than 98 % of open spinal dysraphisms, whereas myeloceles are rare. In contrast, the occurrence of closed spinal dysraphism with Arnold–Chiari II is rare. Associated cranial abnormalities with OSD include tectal beaking, callosal dysgenesis, and subependymal heterotopias.

9.3.1 Closed Spinal Dysraphism

It is also called spina bifida occulta; occulta is the Latin word for "hidden." This old terminology is not appropriate because isolated defects in the posterior elements of the lumbosacral region are found in 10–24 % of the normal population. The term CSD implies unbroken skin. Therefore, this type of dysraphism is not evident at birth and is normally missed prenatally. CSD are usually not associated with Chiari II malformations; therefore, no prenatal surgery is necessary. Embryologically, it results from a failure of fusion or failure of development of part of the vertebral arch, usually its lamina.

- Closed spinal dysraphism (CSD) is usually asymptomatic, with only a small number of children showing concomitant changes of the spinal neuronal tissue.
- CSD are usually not associated with Chiari II malformations; therefore, no prenatal surgery is necessary.
- Disjunction between neural and cutaneous ectoderm during early fetal life, including various mesodermal components such as fibrotic bands with lipomatous tissue, may tether the cord.
- Cutaneous manifestations of an underlying malformation are common.

Lumbosacral skin indentation, hyperpigmentation, nevus, subcutaneous lipoma (Fig. 9.12), patch of hair growth, or dermal sinus are all findings that should prompt further evaluation. Preliminary screening can be performed in newborns with neurosonography, but be aware of the age dependent conus level. The tip of the conus lies between L2 and L4 in babies aged between the 30th and 39th postmenstrual week. On sonography, it is essential to rule out a spinal mass lesion and/or tethered cord. Typically, reduced mobility of the spinal cord and filum terminale associated with an increased thickness of the filum terminale (over 2 mm) suggests cord tethering. In the presence of cutaneous manifestations, MRI and plain films should follow, with or without positive findings in sonography, because this method is very operator dependent.

Although, in the postnatal phase, CSD are mostly asymptomatic; they may cause neurological, urological, and orthopedic problems in children and young adults. These patients typically develop first neurological symptoms at age 3 or during the rapid somatic growth phase (adolescent growth spurt or at school age 4–8 years).

In CSD, focal damage to the spine and its contents can occur during early fetal life. Presumably, the subsequent repair process disturbs the disjunction between neural and cutaneous ectoderm and includes various mesodermal components such as fibrotic bands with lipomatous tissue tethering the cord. The growth of this abnormal mesodermal tissue will lead to a low position of the conus. The mesenchymal

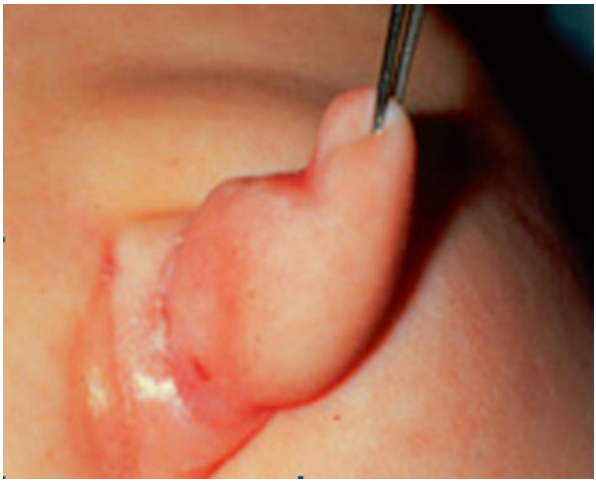

Fig. 9.12 "Taillike" lipoma

origin almost certainly explains the variations of malformations associated with CSD. Therefore, multiple mesenchymal anomalies can be found in the same patient, and these are not limited to the area of the cutaneous manifestations. Adhesions between the cord and dural sac can be caused by a lipoma attached to the filum terminale, by lipomyeloschisis, or by a thickened filum terminale with fibrotic or fat components. Other malformations associated with CSD are split notochord syndrome, terminal myelocystocele, intraspinal enteric cysts, dorsal dermal sinus, and diastematomyelia.

Dermal sinuses are typically oriented from dermal caudal to cranial intraspinal. It has a tract lined by epithelium and can communicate to the central nervous system (CNS) resulting in (Figs. 9.13 and 9.14a) an increased risk for meningitis. Caudal pits at the sacral level and below usually do not communicate with the subarachnoidal space, which ends at the level of S2. The typical dermal sinuses are found more cranially and end intradurally, and these can be associated with dermoid cysts or teratomas. An early surgical intervention is indicated. Otherwise, progressive neurological deterioration results from cord tethering (Fig. 9.13b), epi- or dermoid enlargement (Fig. 9.14b), and compression of the cord or cauda equina. Further possible complications are meningitis and abscess leading to sequelae.

9.3.2 Meningocele

- Closed sac extending through posterior or anterior bone defect.
- MRI is the best method with patient prone not to compress the sac.
- Look for associations: low cord, thick filum terminale, split cord, epidermoid, lipoma, hydromyelia, and Chiari I (Fig. 9.15) are possible due to hydrodynamic imbalance. Also vertebral anomalies: segmentation disorders, hemivertebrae, or Klippel–Feil anomaly.

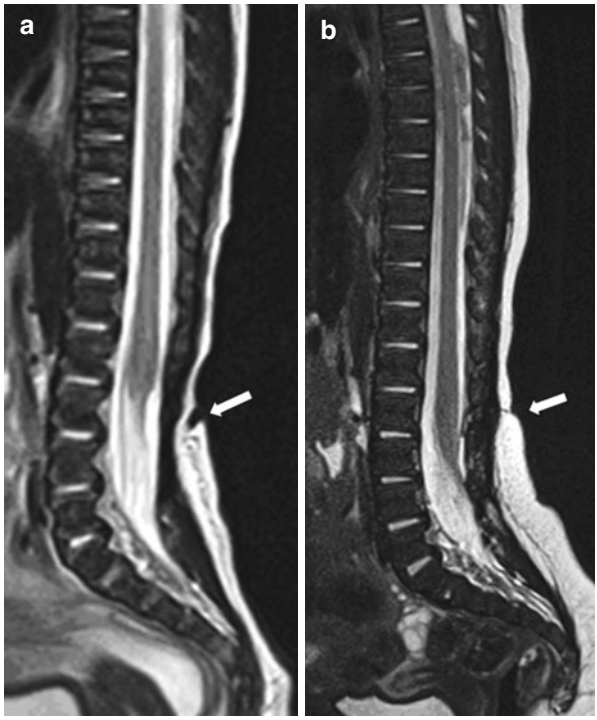

Fig. 9.13 Dermal sinus. (**a**) At 2 days. Sagittal T2-w image MR shows a hypointense linear sinus tract (*arrow*) extending from the skin surface. (**b**) At 7 weeks. After surgery sagittal T2-w image MR shows a much smaller tract (*arrow*) extending from the surface, through posterior elements into the thecal sac. Although the low position of the conus is normal at birth (first MRI image at 2 days), it should have ascended to the normal adult level (L1/L2 interspace) at 7/8 weeks. The persistent low conus at the second image implies tethering; note the adhesion of the conus dorsally

- Look for possible surgical difficulties: entrapped roots attached to the sac, tethered cord, or intraspinal mass outside the sac. Exclude also subcutaneous tracts or fistulas.
- Complications may occur in "simple" meningoceles. Look for malformations!

Note that the simple meningocele (without myelocele) is not associated with Chiari II malformation. It is usually covered by a layer of epidermis covering the meninges. Therefore, no increase in the AFP is seen.

The meningocele is more common at the lumbar and sacral locations but can also occur at the cervical level (Fig. 9.15). In fact, it can be found anywhere along the spine. The frequency of meningocele is 1 in 10,000 births.

Because this kind of lesion does not involve the spinal cord, no neurological symptoms are present. Treatment usually follows due to cosmetic reasons. Meningocele is lined by arachnoid; in this way, arachnoid adhesions may obstruct the neck of the sac. The CSF-filled sac herniates through a posterior spinal defect, but the spinal cord does not enter the sac. Occasionally, the filum terminale or nerve roots herniate (Fig. 9.16).

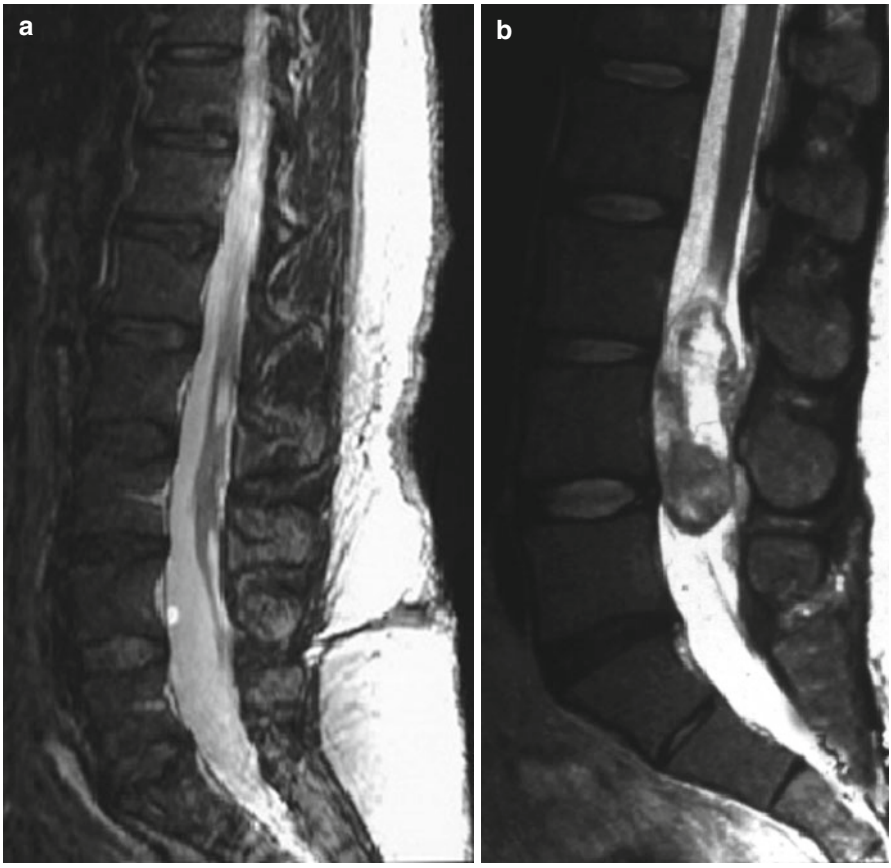

Fig. 9.14 Dermal sinus and dermoid. (**a**) Patient **a**: Sagittal T2-w image MR demonstrates lumbar skin dimple (*white arrow*) with a persistent connection, dermal sinus tract containing a small dermoid (*black arrow*). The low-lying spinal cord is fixed to dorsal lipoma (*block white arrow*). (**b**) Patient **b**: Sagittal T2-w image MR shows a heterogenous, mixed intensity mass in the region of conus medullaris und cauda equina. Note the expanding of the cord. The hyperintensity (*block white arrow*) was due to fat in the dermoid

9.3.2.1 Lipomyelomeningocele

- Mesenchyme is incorporated into neural folds.
- Twenty to fifty-six percent of CSD. Not associated with Chiari II. The brain is typically normal.
- The deep portion of the lipoma is adherent to the placode, but the roots do not travel through the lipoma.
- MRI evaluation should assess the relationship between lipoma and neural placode. Rule out any central canal extension of the lipoma. Position of lipoma, placode, and nerve roots in relation to the midline.
- Rule out cord tethering, myeloschisis, terminal hydromyelia.
- Look for possible surgical difficulties: specially rotation of the lipoma with secondary distortion of the nerve roots.

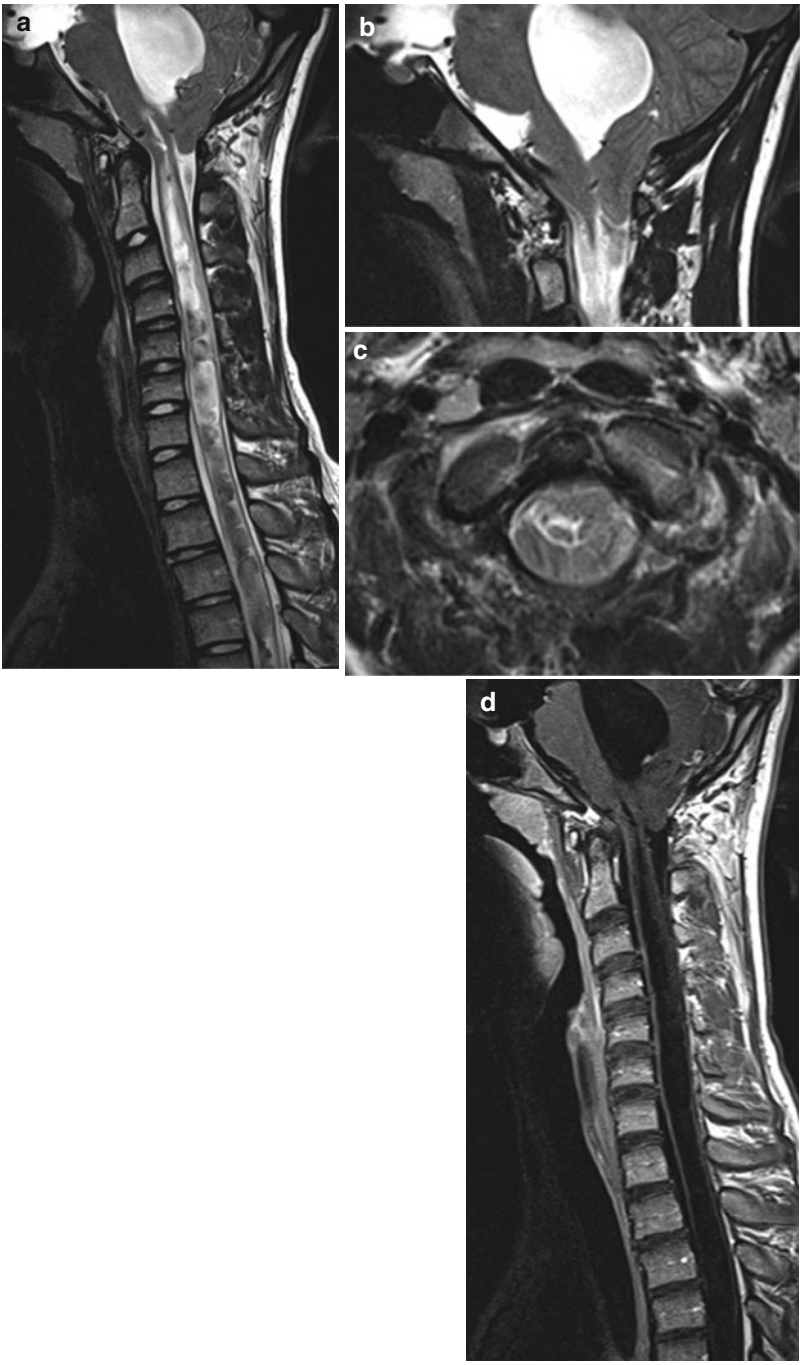

Fig. 9.15 Chiari I malformation. (**a**) Sagittal T2-w image shows herniation of the cerebellar tonsils through the foramen magnum into the cervical spinal canal. There is a large distention of the central canal of spinal cord filled with CSF (i.e., hydromyelia), and also hydrocephalus with the enlarged fourth ventricle is seen. (**b**) The cerebellar tonsils are elongated, and a mild kinking of the medulla is present. (**c**) The tonsillar herniation fills the cisterns. (**d**) Contrast-enhanced T1-w images should be performed to exclude a tumor

Fig. 9.16 Cervical meningocele. Sagittal T1-w image shows nerve roots herniating into sac (*white arrow*). This dysraphism is close and therefore not associated with Chiari II malformation

Re-tethering

The diagnosis of re-tethering after surgery is clinical; MRI is indicated to rule out complications.

The neural tube forms by infolding and closure of neural ectoderm as it separates from cutaneous ectoderm during the third and fourth weeks. Lipomyelomeningocele is probably a result of premature disjunction. The mesenchyme is exposed with contact to the neural tube. As a consequence, the ependymal lining of the primitive neural tube induces the mesenchyme to form fat. The neural folds remain open, forming a neural placode at the site of premature disjunction. It accounts for 20 % of the skin-covered lumbosacral mass. Unfortunately, lipomyelomeningocele's incidence is not reduced with the supplementation of folate.

Fig. 9.17 Lipomyelomeningocele: sagittal T2-w image reveals an elongated, tethered low-lying spinal cord inserting into a large terminal lipomatous mass contiguous with subcutaneous fat through dysraphic defect

The deep portion of the lipoma is adherent to the placode (Fig. 9.17). The lipoma may spread superiorly along the myeloschisis and may involve the spinal cord. Almost always, there is a low position of the involved spinal cord (Fig. 9.17) which ends at the placode. The roots do not travel through the lipoma. Instead, the motor and sensory roots exit from the ventral surface. With larger meningoceles, the lipoma, which is tethered to the cord, may rotate and then cause distortion of the nerve roots. The repair in the case of asymmetrical lipomas can be difficult with short nerve roots on the lipoma side and elongated roots on the other side, necessitating careful relocation at surgery.

If left untreated, these children usually show irreversible progressive neurological impairment (16–88 %) due to cord tethering and enlarging lipoma (the lipoma grows with the infant). If tethering of the cord is not released early, bladder dysfunction usually persists. The main goal of reconstructive surgery is to untether the spinal cord, to reduce the volume of the lipoma, and to reconstruct the spinal canal, at the same time minimizing scarring and, consequently, the risk of re-tethering. Postoperatively, patients should not deteriorate with longitudinal growth. It is important to know that symptomatic re-tethering is common, weeks or years after surgery.

Imaging
The high signal of lipomas, contrasting to the intermediate signal of the cord, gives an excellent contrast in sagittal and axial T2-w images (Fig. 9.17). T1-w with and without spectral fat suppression confirms the fatty composition of the mass. The most common differential diagnosis is intradural and terminal lipomas. The former, also called juxtamedullary lipoma, is covered by an intact dura, and cutaneous manifestations are unusual.

9.3.2.2 Split Cord Malformation

- Diastematomyelia: spinal cord or canal splitting
- Diplomyelia: RARE, spinal cord or canal duplication; each cord with two anterior and two posterior horns and roots
- Rule out in patients with cutaneous stigmata ("faun's tail" hair patch), intersegmental fusion of posterior elements, and clinical tethered cord
- Look for spur: almost pathognomonic for split cord malformation (SCM): intersegmental laminar fusion + segmentation anomalies
- While osseous spur are visible, fibrous spurs may be occult.

Split cord malformations (SCM) include both diastematomyelia (diastema from ancient Greek means spacing) and diplomyelia. Diastematomyelia (Fig. 9.6) is distinguished from the rare diplomyelia, a more or less complete duplication of the spinal cord. In diplomyelia, there are two separate whole cords, each with two ventral and two dorsal nerve roots.

In the case of diastematomyelia, there is a sagittal division of the cord. Usually, only a short segment is involved with asymmetry in size of the hemicords, each segment is lined by its own pia mater, and each hemicord has a central canal. The cleft can be complete or it may involve only the ventral or dorsal half of the cord. The septum between the two pia-lined hemicords can be an ossified spur (type I, Fig. 9.18c), or a non-ossified fibrous septum can be present within a single dural tube (type II, Fig. 9.6b). This last type is rarely symptomatic, unless hydromyelia and tethering are present.

The length of the split cord is variable and, by necessity, longer than the spur. The cleft is between T9 and S1 in 85 % of the cases. The classical bone spur is not always found in all patients with SCM; patients may present with a partial or complete fibrous bridge between the posterior surface of the vertebral body and the vertebral arch. Hemicords usually reunite below the cleft (ca. 90 %). It should be noted that the spur arises from the laminae and afterward fuses with the vertebral body. Therefore, asymmetry of the two canals may result from the oblique position of the spur or from scoliosis, which rotates the spur.

SCM are usually associated with vertebral body anomalies, such as segmental and fusion anomalies, intersegmental laminar fusion associated with spina bifida (60 %), myelocele/myelomeningocele (15–25 %), hemimyelocele (15–20 %), tethered cord (75 %), thickened filum terminale (40–90 %), hydromyelia (50 %) in one or both hemicords (often above the diastematomyelia), scoliosis (79 %), and Chiari II malformations (15–20 %).

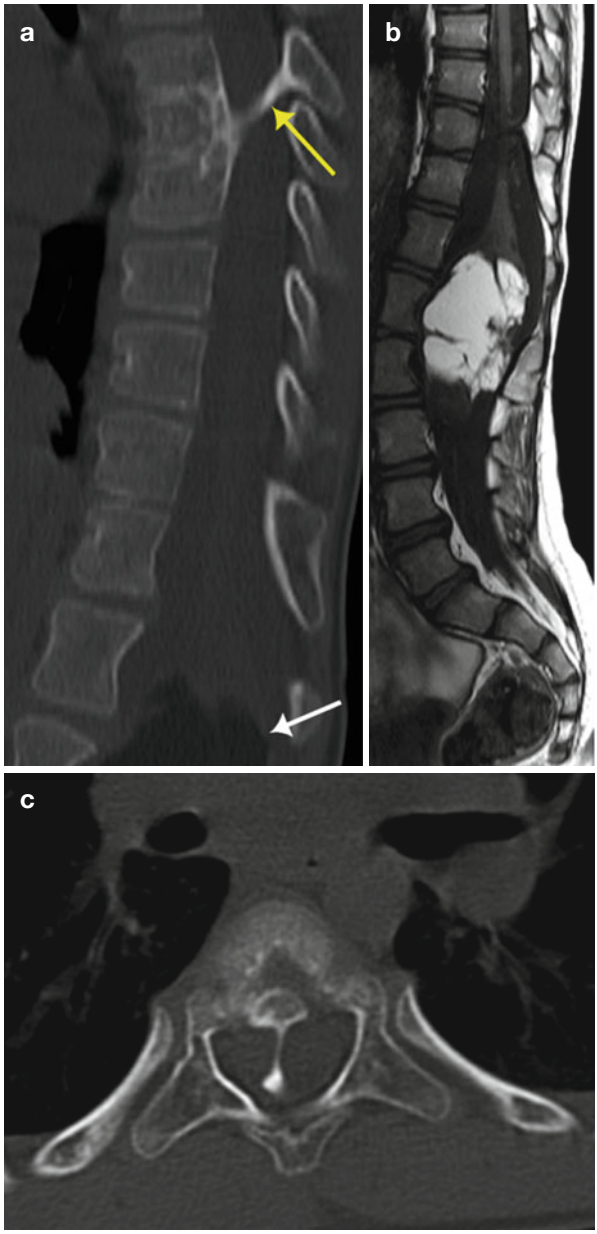

Fig. 9.18 Diastematomyelia with lipoma. (**a**) CT shows bony diastematomyelia (*yellow arrow*) at the upper spine with bony remodeling at the level of the lipoma (*white arrow*). (**b**) Sagittal T1-w image shows a hyperintense mass in the region of the conus medullaris, partially intramedullar. The T1 hyperintensity suggests dermoid or an intradural (juxtamedullary) lipoma. (**c**) The axial CT image shows a large osseous spur dividing the canal

Imaging

MRI is necessary to detect the extension of the cord split, to assess the existence of a fibrous septum and hydromyelia, to determine the level of the conus and to rule out other causes of tethering. It is important to evaluate the nerve roots, which can become adherent to dura and tether the cord. Computed tomography (17C) may show ossified septation and can be very useful for surgical planning.

9.3.2.3 Terminal Myelocystocele

Important points
- Closed sac with marked cystic dilatation of the distal cord central canal or the *ventriculus terminalis*
- MRI is the best method for patients not prone to compress the sac.
- Look for associations: hydromyelia with low-lying tethered cord. Not associated with Chiari II malformation
- MRI is performed to determine the extension of hydromyelia and rachischisis and the size of the cysts and to rule out associated anomalies.

Terminal myelocystocele (Fig. 9.9) is a skin-covered uncommon malformation. The distal central canal becomes noticeably dilated and herniates through a posterior lumbosacral defect. It may represent a large persistent terminal ventricle. This anomaly can be difficult to be differentiated from meningomyelocele (MMC) prenatally. Distinguishing myelocystocele from the former, the presence of a thick-walled sac (skin cover), the absence of a true neural placode dorsally, the absence of Chiari II malformation, and the lack of elevated AFP in the maternal blood suggest this diagnosis.

MRI rules out genitourinary malformations. Notably, myelocystocele can be associated with caudal regression syndrome and OEIS syndrome (omphalocele, exstrophy of the bladder, imperforate anus, and spinal anomalies).

The ballooning of the terminal ventricle disrupts the mesenchyme, but not the ectoderm (Fig. 9.9c, d). At the same time, the cyst volume prevents the ascent of the cord with tethered cord.

9.3.3 Open Spinal Dysraphism

This entity is commonly located in the lumbosacral region (80–90 %), a location associated with the final component of neural tube closure. The incidence of OSD is of 0.5–1 in 1,000 live births. Typically, it presents with an increased interpeduncular distance, wide spinal canal, and absence or incomplete closure of the vertebral arches. Other neurological defects may be associated in the patient, such as hydrocephalus, diastematomyelia, Arnold–Chiari malformation, hydromyelia, or a tethered spinal cord.

Meningomyelocele

- Open sac extending through posterior bone defect. Neural tissue, meninges, and CSF exposed
- Initial MMC diagnosis with obstetrical ultrasound

- Fetal MR: eligibility for fetal surgery
- Antenatal diagnosis
- Look for open neural arch, MMC sac, and Chiari II findings.
- Rule out associated anomalies: hydrocephalus, diastematomyelia, Chiari II, hydromyelia, or a tethered spinal cord. Important: (1) Diastematomyelia can occur at a higher level than the MMC! (2) Syringohydromyelia may develop and produce late-onset symptoms!
- Low conus on MR imaging is not always a sign of clinical tethering!
- MRI: postoperative clinical deterioration requires craniospinal reevaluation.
- Important: re-tethering of the spinal cord with adhesions to the dura is always present; therefore, it is of questionable diagnostic significance.

Meningomyelocele is the most common form of OSD. It involves the spinal cord and meninges and may be covered by a thin layer of skin or by a membranous sac. Clinically, these patients present with limb paralysis, bladder and bowel incontinence, or dislocations of the hip. Other potential associated abnormalities are hydromyelia, split cord with or without diastematomyelia (Figs. 9.6b and 9.18c), hydrocephalus, Arnold–Chiari malformations (Fig. 9.11) or scoliosis, kyphosis, or lordosis. Congenital scoliosis and kyphosis are found in approximately 30 % of the patients with MMC and are due to associated anomalies, such as hemivertebrae (Fig. 9.10), bony spurs, and unilateral fusions. Developmental scoliosis and kyphosis are present in 30 % of the patients resulting from muscular imbalance.

Sometimes, as a result of the neural tube not closing properly, the spinal cord is exposed, also called myeloschisis. This is the most severe type of spina bifida, and it bears the risk of severe infection. The nervous structures remain as a placode; its ventral surface is lined by pia-arachnoid. The nerve roots arise directly from the ventral surface (Fig. 9.19c). Dorsally the neural placode is freely exposed. Leaking of the cerebrospinal fluid (CSF) is common because of rupture of the thin subarachnoidal membranes.

Advances in prenatal ultrasound and MRI have significantly improved the diagnosis and therapy of spinal dysraphism prenatally. Screening should be performed with ultrasound. In addition, fetal MRI has significantly improved in the recent years and is an excellent tool in the complementary evaluation of the spinal malformation and associated CNS anomalies. Both methods contributed to the evaluation of the malformation, determining the need for in utero surgery. It appears that surgery covering the exposed spinal cord in utero preserves the distal neurological function, due to the reduced chemical irritation caused by amniotic fluid exposure. In addition, in cases treated prenatally, there was a reduction of hindbrain herniation with decreased need for ventricular shunting in some of the cases. Therefore, MRI plays a significant role in confirming the ultrasound findings, making the correct diagnosis, and ruling out additional anomalies and to decide about the eligibility for fetal surgery in case of MMC.

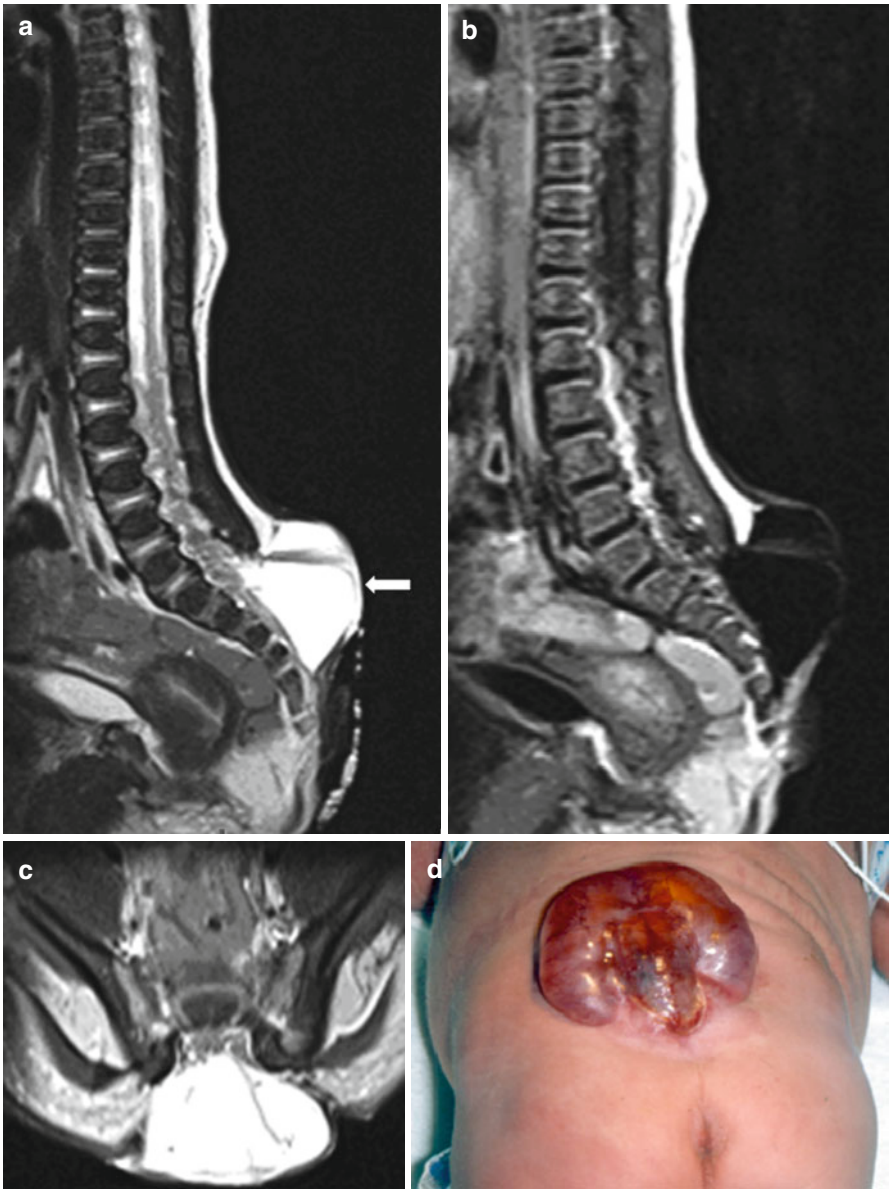

Fig. 9.19 Myelomeningocele. (**a**, **b**) Sagittal T2-w and T1-w images show, respectively, an unrepaired sacral myelomeningocele with open spinal dysraphism, CSF-filled myelomeningocele sac, and dorsal placode (*white arrow*). (**c**) The axial T2-w image confirms the dysraphism. The nervous structures remain as a placode with the nerve roots arising directly from its ventral surface. (**d**) Another patient. Note that the neural placode is freely exposed with leaking of CSF. The closure has to be performed during the first 48 h to prevent infection

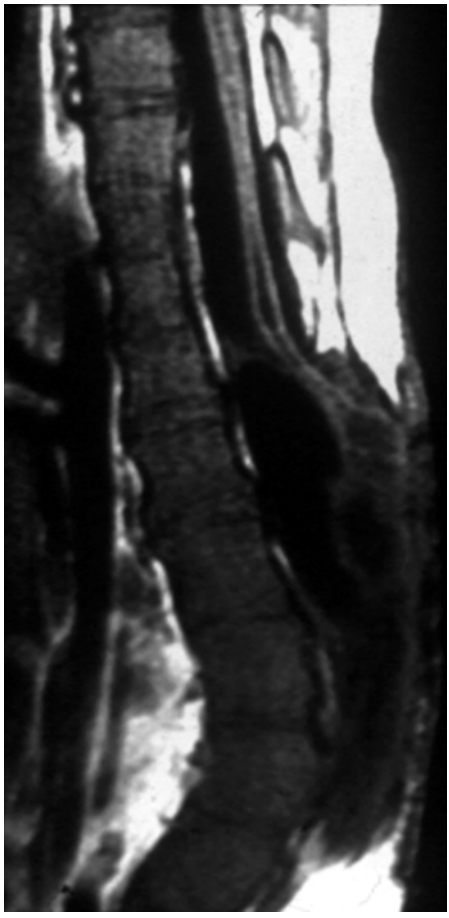

Fig. 9.20 Myelomeningocele after repair. Normal aspect with re-tethering of the cord, scar, and adhesions to the dura. Note the new development of syringohydromyelia, which explains neurological deterioration in this patient

After birth, the diagnosis of OSD is clinically easy (Fig. 9.19d), and imaging untreated MMC is questionable. If indicated, the aim of MRI is to evaluate the malformation in detail and to rule out associated anomalies prior to corrective surgery. Associated anomalies, such as diastematomyelia at a higher level than the MMC, indicate that a more extensive surgery will be necessary.

The best possible outcome in these patients is a stable postoperative deficit. Patients with MMC, who after surgery or later in life show clinical neurological deterioration, should be reevaluated with MRI. The aim is to detect postoperative complications (e.g., constriction secondary to dural ring by scar), concomitant unrecognized abnormality (e.g., split cord with or without diastematomyelia) or changes in the malformation. For example, syringohydromyelia (Fig. 9.20) may develop (29–77 %) and give late symptoms. Other possible postoperative complications are arachnoid cysts, dermoids or inclusion tumors, or cord ischemia. Re-tethering of the spinal cord with adhesions to the dura (Fig. 9.19) is always present and, therefore, is of questionable diagnostic significance.

9.4 Miscellaneous Malformations of the Spine

9.4.1 Tethered Cord and Fibrolipomas of the Filum Terminale

- Thickened filum terminale: >2 mm at L5–S1 level.
- Tethered cord: conus tip below the level of the L2 vertebral body + tethered by thickened filum.
  Usually, patients present with combination of both the above. However, tethered cord may occur without thickened filum, or the filum is thickened, but the conus lies in its normal position. In these cases, it is helpful to evaluate the position of the conus medullaris: it lies dorsal (even in prone position) in tethered cord.
  Important: *tethered cord is a clinical diagnosis*. It can be present regardless of normal conus position and normal thickness of the filum.
- Low-lying conus can present as a normal variant without symptoms.
- Lipomas: incidental findings in 4–6 % of exams.
  MRI: sagittal images alone should not be used to diagnose tethering.
  Look for CSD, hydromyelia, myelomalacia, lumbosacral hypogenesis, and VACTERL syndrome.

The filum terminale is a long and thin (under 2 mm at L5–S1 level) filament. The thickened filum terminale is defined as an enlargement of the filum to a diameter of 2 mm or more at the L5–S1 level. Tethered cord is described as the conus tip below the level of the L2 vertebral body associated with thickened filum terminale und dorsal position of the conus medullaris (even in prone position).

Tethered cord results from an incomplete regressive differentiation with failure of the terminal cord involution or failure of filum terminale to lengthen. The conus should be in the adult normal position (at or above the level of the L2 vertebral body) at the latest by 2 months of age. Lipoma of the filum (Fig. 9.20) can result from minor alteration in the canalization and regression. Note though that lipomas are found as incidental findings in 4–6 % of normal spinal exams.

Patients usually present with a combination of tethered cord and thickened filum terminale. However, tethered cord may occur without thickened filum or the other way around (the filum is thickened, but the conus lies in its normal position). A significant number of patients present with clinical symptoms of tethered cord but on MRI show normal filum diameter and normal conus position. This does not preclude the diagnosis of tethered cord. Conversely, low-lying conus can be present as a normal variant without symptoms. In these patients, prophylactic surgery is controversial. Physiologically, the tethering impairs the oxidative metabolism of conus and nerve roots with secondary abnormal lumbosacral function.

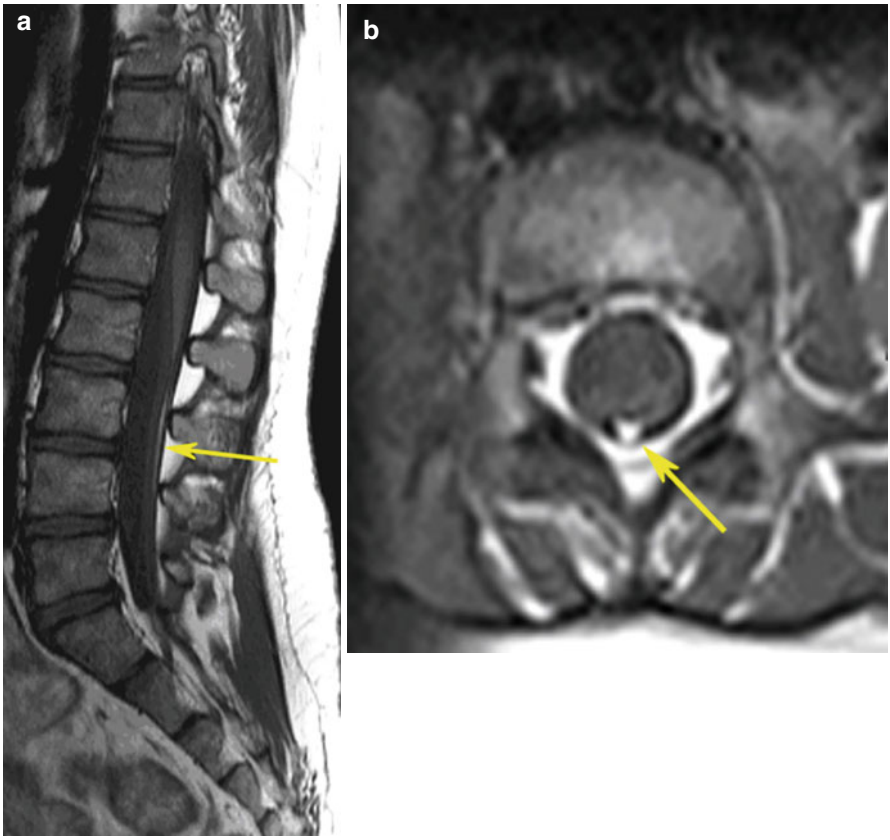

Fig. 9.21 Lipoma with tethered cord. (**a**) Sagittal T1-w MR shows borderline low-lying conus (at the inferior L2 vertebral level). The filum (*yellow arrow*) contains fat. (**b**) Axial T1-w MR confirms the presence of fat in filum terminale (*yellow arrow*)

However, while the filum is usually thickened by fibrosis (55 % of abnormal cases), in ca. 20 % of the cases, a thin lipoma is found (Fig. 9.20) or rarely a filar cyst. Tethered cord is commonly associated with cutaneous stigmata, CSD (33–100 % depending on the references), hydromyelia, myelomalacia, and scoliosis. Clinically, it typically becomes symptomatic during adolescent growth, but symptom onset has been described as early as 3 years of age and as late as 76 years of age.

Imaging

Neurosonography can be used in the diagnosis if the child is less than 6 months old; the findings need to be confirmed with MRI. On MRI, the dural sac is usually widened with dorsal positioning of the conus (even when the patient is scanned in a prone position), and the thickened filum is attached to the dorsal dura. Filum lipoma appears as high signal on T1-w images. When the filum is thickened by dense fibrosis, it has a signal appearance similar to the nerve roots (Fig. 9.21b). It is important to emphasize

that sagittal MR images alone should not be used to diagnosis tethering. The exact location of the conus should be determined on axial scans, in which the filum appears as a low signal structure within high signal CSF. If evaluated on the sagittal images, the cauda equina may lead to an ambiguous evaluation of the conus tip.

After surgery, the recurrence of symptoms is rare; if present, a new MRI evaluation is required to rule out re-tethering.

9.4.2 Caudal Regression Syndrome

Abnormal distal spinal cord associated with lumbosacral dysgenesis/agenesis. It can be divided into:

- Group one: severe sacral osseous anomalies and dilated central spinal canal. Abrupt termination of the cord above L1
- Group two: the cord is tapered, low lying, and elongated with tethering, and a spinal lipoma may be present.

Differential diagnosis: tethered spinal cord, no caudal dysgenesis
Rule out tethered cord in all patients with caudal dysgenesis, even in the mild case of an absent coccyx.
Look for genitourinary and anorectal malformations in patients with CRS.

Caudal regression syndrome (CRS) is characterized by sacral dysgenesis (Fig. 9.22) associated with genitourinary and gastrointestinal malformations. Sacral agenesis/dysgenesis is a rare congenital anomaly of the spine, and the incidence is 1/7500 births, mostly milder forms of dysgenesis. In 15–20 % of the cases, the mother has diabetes, but most cases are sporadic. The embryogenesis of this syndrome is still controversial. Patients with a deranged caudal development of the spine, which includes canalization and regression, will show tethered cord with or without dysgenesis of the cord associated with caudal vertebral agenesis. The second group with disruption prior to the fourth gestational week presents with agenesis of parts of the end of the spinal cord, spinal ganglia, and spine. This suggests that the primary neurulation is involved with abnormal neural tube and notochord development (Fig. 9.23).

Morphologically, it presents as a spectrum varying from a mild form with an absent coccyx to a severe form and complete lumbosacral agenesis. It can also present as a unilateral sacral agenesis/dysgenesis with oblique lumbosacral joint, pelvic tilt, and scoliosis. In the case of a bilateral lumbosacral agenesis, the vertebral column terminates at the level of the thoracic spine, and the lowest vertebra articulates with the ilia. Alternatively, the ilia are fused below the lowest vertebrae.

The MR findings in CRS can be divided into two groups. The first is characterized by distal spinal cord hypoplasia; the distal spinal cord typically terminates abruptly in a “wedge-shaped” form. In this case, the dorsal portion of the cord extends more caudally than the ventral portion (Fig. 9.22). Usually, the caudal roots extend downward vertically; it looks like a distal focal “diastematomyelia” is present arising from

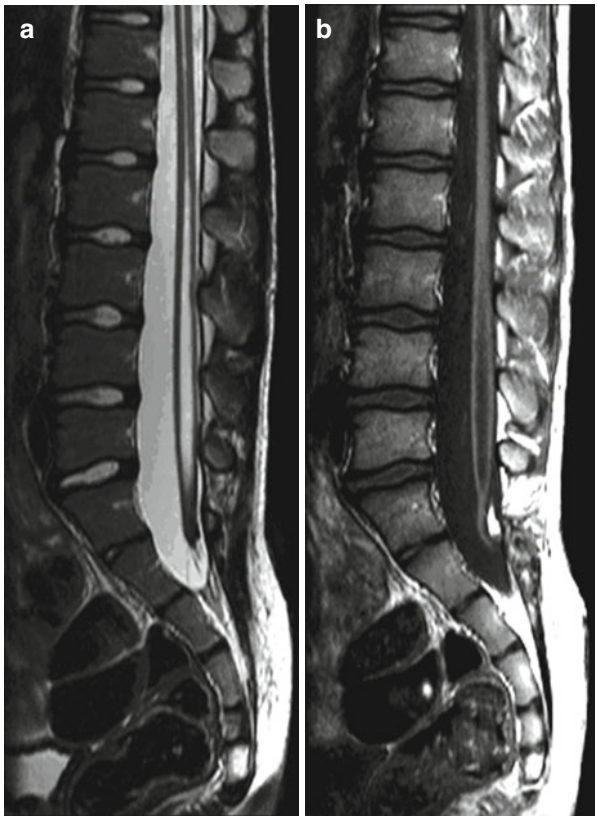

Fig. 9.22 A 8 years old boy with typical tethered cord. (**a**) Sagittal T2-w reveals a low-lying hydromyelic tethered cord with fibrolipoma (*curved white arrow*) inserting into a terminal lipoma. Marked signal loss at S1/S2 level compatible with lipoma. (**b**) Sagittal T1-w MRI shows an elongated low-lying hydromyelic spinal cord extending to the S1 level, ending in a small terminal lipoma (*block white arrow*). Notice above the level of the lipoma, the subcutaneous fat extending through the dorsal dysraphism (*straight white arrow*)

the dysplastic conus with a gap between the anterior and posterior roots. This group of patients usually present with severe sacral osseous anomalies and dilated central spinal canal. In the second group of patients, the cord is tapered, low lying, and elongated with tethering, and a spinal lipoma may be present. The main differential diagnosis is tethered spinal cord, in which patients present no caudal dysgenesis.

There is an association with VACTERL (10 %), which is a nonrandom association of birth defects (V, vertebral; A, anal; C, cardiac; TE, trachea/esophagus; R, renal; and L, limbs). Cardiac anomalies may be present in 24 % of these patients. The lower extremities are often affected; the extreme case with fusion of the lower extremities is called sirenomelia. The peritoneal and gluteal muscles are hypoplastic with fat infiltration. An imperforated anus or anal atresia is frequent. MRI may show not only the anorectal anomalies but also the genitourinary (24 %; such as renal agenesis, ectopia, hydronephrosis, bladder malformations) anomalies and can analyze the pelvic musculature.

A tethered cord is present in all patients with CRS, in whom the conus terminates below L1. Other spinal anomalies may include vertebral anomalies (22 %), lipo- and myelomeningocele (10–50 %), hydromyelia (10 %), diastematomyelia, terminal myelocystocele (15 %), and anterior sacral meningocele.

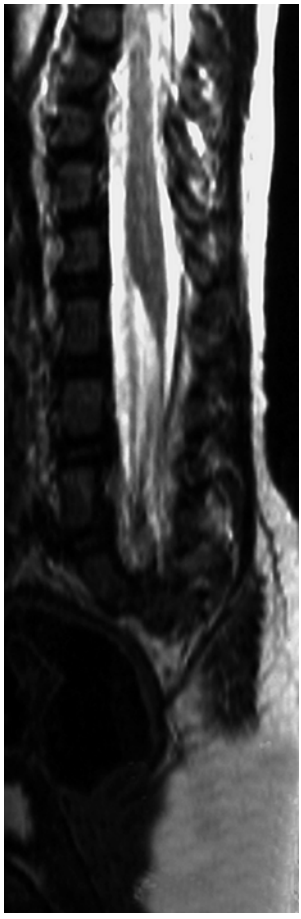

Fig. 9.23 Caudal regression syndrome with sacral agenesis and multiple vertebral segmentation anomalies. Sagittal T2-w image shows that the dorsal portion of the cord extends more caudally than the ventral portion

Further Reading

1. Bulas D (2010) Fetal evaluation of spine dysraphism. Pediatr Radiol 40:1029–1037
2. Chen YF, Liu HM (2009) Imaging of craniovertebral junction. Neuroimaging Clin N Am 19:483–510
3. DeLaPaz RL (1993) Congenital anomalies of the lumbosacral spine. Neuroimaging Clin N Am 3:425–442
4. Ghanem I, El Hage S, Rachkidi R, Kharrat K, Dagher F, Kreichati G (2008) Pediatric cervical spine instability. J Child Orthop 2:71–84
5. Lustrin ES, Karakas SP, Ortiz AO, Cinnamon J, Castillo M, Vaheesan K, Brown JH, Diamond AS, Black K, Singh S (2003) Pediatric cervical spine: normal anatomy, variants, and trauma. Radiographics 23:539–560
6. Smoker WR (1994) Craniovertebral junction: normal anatomy, craniometry, and congenital anomalies. Radiographics 14:255–277